1974

The effects of surface roughness on waveguide-mode propagation

Jose A. Azarcon Jr.
Iowa State University

INFORMATION TO USERS

This material was produced from a microfilm copy of the original document. While the most advanced technological means to photograph and reproduce this document have been used, the quality is heavily dependent upon the quality of the original submitted.

The following explanation of techniques is provided to help you understand markings or patterns which may appear on this reproduction.

1. The sign or "target" for pages apparently lacking from the document photographed is "Missing Page(s)". If it was possible to obtain the missing page(s) or section, they are spliced into the film along with adjacent pages. This may have necessitated cutting thru an image and duplicating adjacent pages to insure you complete continuity.

2. When an image on the film is obliterated with a large round black mark, it is an indication that the photographer suspected that the copy may have moved during exposure and thus cause a blurred image. You will find a good image of the page in the adjacent frame.

3. When a map, drawing or chart, etc., was part of the material being photographed the photographer followed a definite method in "sectioning" the material. It is customary to begin photoing at the upper left hand corner of a large sheet and to continue photoing from left to right in equal sections with a small overlap. If necessary, sectioning is continued again — beginning below the first row and continuing on until complete.

4. The majority of users indicate that the textual content is of greatest value, however, a somewhat higher quality reproduction could be made from "photographs" if essential to the understanding of the dissertation. Silver prints of "photographs" may be ordered at additional charge by writing the Order Department, giving the catalog number, title, author and specific pages you wish reproduced.

5. PLEASE NOTE: Some pages may have indistinct print. Filmed as received.

Xerox University Microfilms
300 North Zeeb Road
Ann Arbor, Michigan 48106

The effects of surface roughness on waveguide-mode propagation

by

Jose A. Azarcon, Jr.

A Dissertation Submitted to the
Graduate Faculty in Partial Fulfillment of
The Requirements for the Degree of
DOCTOR OF PHILOSOPHY

Major: Electrical Engineering

Approved:

Signature was redacted for privacy.

In Charge of Major Work

Signature was redacted for privacy.

For the Major Department

Signature was redacted for privacy.

For the Graduate College

Iowa State University
Ames, Iowa

1974

TABLE OF CONTENTS

LIST OF SYMBOLS

a_m	mode attenuation, decibels per kilometer (dB/km)
Ai	Airy integral function
B	$2k^2K$, per meter^3
B'	$B^{1/3}$, per meter
c'	equivalent complex dielectric constant of rough surface
C	cosine of complex angle of incidence at ground
$\bar{E}$	electric field intensity, volts per meter
F_{rs}	rough-surface reflection factor
h	surface roughness characteristic height (rms), meter
H	duct height, meters
$\bar{H}$	magnetic intensity, amperes per meter
j	stratum or layer number
k	wave number, per meter
K	lapse rate of refractive index, per meter
K_1	lapse rate of refractive index inside duct, per meter
K_2	gradient of refractive index for standard atmosphere, per meter
m	mode order
M	refractive modulus
n	refractive index
N	refractivity = $(n - 1) \times 10^6$

R	Fresnel reflection coefficient of plane surface
R'	Fresnel reflection coefficient of equivalent surface
u	complex variable
u'	$u\exp(-j2\pi/3)$
W	duct depth, meters
X	$\sigma/\omega\varepsilon = 60\sigma\lambda$
z	vertical distance from ground level, meters
Z_g	effective ground surface impedance, ohms
ε	permittivity, farads per meter
μ	permeability, henrys per meter
σ	conductivity, mhos per meter
η	characteristic impedance of ground, ohms
Θ	angle of incidence, radians
Φ	grazing angle, radians
λ	wavelength, meters
ω	frequency, radians per second

INTRODUCTION

When the atmospheric conditions are such that the refractive index of the air decreases with height, as is frequently the case in shallow but horizontally extended regions of the troposphere, decimetric and shorter radio waves can undergo pronounced refraction and thus be trapped within these layers and guided along the surface of the earth. This results in intense fields near the surface of the earth, far exceeding those obtained under "normal" conditions. This propagation mechanism, referred to variously as waveguide-mode or duct propagation or trapping, depends upon rather minute changes in refractive index; refractive index contrasts as small as 5 N units ($N = (n - 1) \times 10^6$, where n is the radio refractive index of the atmosphere) are capable of supporting modes in the upper VHF band. Frequencies extending up to 1000 gigahertz are influenced by refractive gradients in the atmosphere. This difference can be attributed to the ability of the polar molecules of water to respond to the electrical stimulus supplied by a passing radio wave.

The waveguide mode of propagation was first recognized more than fifty years ago as the mechanism for long-distance trans-oceanic radio communication, having been suggested by Watson(1,2) in 1919. Watson proposed that high-frequency waves propagate between the earth and the ionosphere in a

manner analogous to that in parallel-plate waveguides, with waves being reflected successively from the earth and ionosphere. Numerous observations of "anomalous" propagation effects were reported in the late thirties and early forties and included such phenomena as greatly extended propagation distances, severely reduced ranges, as well as improved television reception at twilight and early evening hours. A considerable amount of theoretical and experimental effort was devoted to atmospheric refraction during World War II in view of the military applications and significance of the phenomenon. The book edited by D. E. Kerr(3) and the report of the British Physical Society in 1948, "Meteorological Factors in Radio Wave Propagation"(4), represent a summary of the wartime effort on the part of the Americans and British, respectively. T. L. Eckersley(5), with Millington(6), contributed a great deal to the development of the theory of tropospheric refraction. The full impact of the work of these two researchers was not entirely appreciated during their time, however, due in part to the allegedly difficult style in which they wrote. Budden(7) further developed the ideas of tropospheric refraction in a monograph published in 1960; his book is a particularly fine introduction to the subject of mode propagation. In many ways, the subject of atmospheric refraction has been well-studied. It is significant, however, that until now, investigators have only

glossed over the effects of surface roughness and the finite conductivity of natural surfaces in the short-wavelength portion of the radio spectrum. For this reason, this work will attempt to extend the theory and methods of radiowave propagation in the atmosphere in order to assess the effects of the above-mentioned parameters in the propagation mechanism.

Before going into the solution of the mode problem itself, a brief introduction to the meteorological elements of the problem and the basic theory of waveguide-mode propagation will be made.

The refractivity of a well-mixed parcel of air, having temperature T and pressure p has been empirically described in the following equation:

$$N = (n - 1)\times 10^6 = \frac{A}{T}(p + Be/T) \qquad (1.1)$$

where e = partial pressure of water vapor, mb
A = 79°K/mb
B = 4800°K
n = n(z), the refractive index of air

In wave propagation studies, the form given above is commonly used; in meteorology, the usual unit is the refractive modulus M,

$$M = [n(1 + z/a) - 1]\times 10^6$$

or

$$M = N + (z/a)\times 10^6 \qquad (1.2)$$

where $N = (n - 1)\times 10^6$
$n = n(z)$, the refractive index of air at height z
a = radius of the earth

The term z/a is a correction factor for the actual refractive index of the atmosphere and is used in an earth-flattening procedure whereby the relative curvature between the earth and a radio ray is maintained when the earth is "flattened" ($a \to \infty$) and the air replaced by a fictitious medium with the refractive index $(n + z/a)$. A detailed derivation of this procedure may be found in Pekeris(8).

Examination of equation (1.1) will show that the refractive index may decrease with height according to the following changes in the parameters T and e:

(a) decrease in water-vapor pressure

(b) increase in air temperature

These meteorological events occur when there is advection, subsidence, radiation, or a combination of these processes (9, pp. 132-134). The occurrence of radio ducts under these conditions is fairly regular in a temporal sense and has been observed in tropical, subtropical, and temperate regions of the world.

Due to the constant mixing taking place in the atmosphere, there are two observable patterns in the vertical profile of refractive index. First, there is the fine-scale fluctuation pattern due to relatively high gradients occurring over distances which are short compared with a wavelength. The other pattern is the gross, or large-scale, variation to which the incidence of radio refraction is attributed by current theory. These variations in the refractive index as a function of height are depicted below in a replica of a profile taken with airplane-borne instrumentation (Figure 1.1).

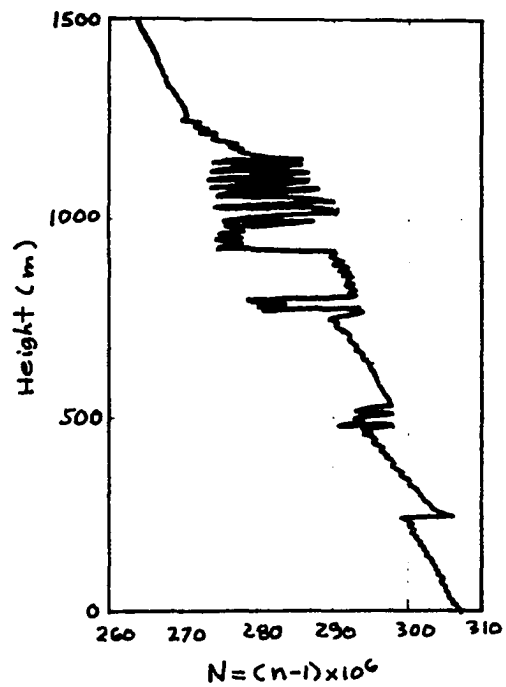

Figure 1.1. Replica of an actual refractive index profile taken by instrumentation in an airplane. (from du Castel(10)).

Conventionally, radio ducts may be classified according to their location with respect to the surface of the earth, as shown in figure 1.2. In these schematic representations of the average refractive index profile, the corresponding graphs of the temperature and humidity are included. A great variety of these types of graphs are to be found in references 3, 9, and 11.

In this paper we will consider surface ducts alone, since these might be expected to be affected by surface conditions, so that all types of SS and ES ducts should be included for completeness. Of the latter kind, those cases in which the duct depth W is low enough so that the downgoing component wave of a mode actually reaches the ground are important but these will not be considered here. Wait and Spies(12) and Chang(13) have published some analyses of elevated tropospheric ducts. Their use of the linear-segmented profile technique is an important feature of the work to be described herein.

In metallic waveguides, waves travelling along the guide axis can be represented by crossing pairs of component waves. The discrete number of these pairs ("modes") depends upon the spacing between the guide walls and the wavelength of the field. At either wall, each component wave will have its wave normal making an angle ϕ with respect to the

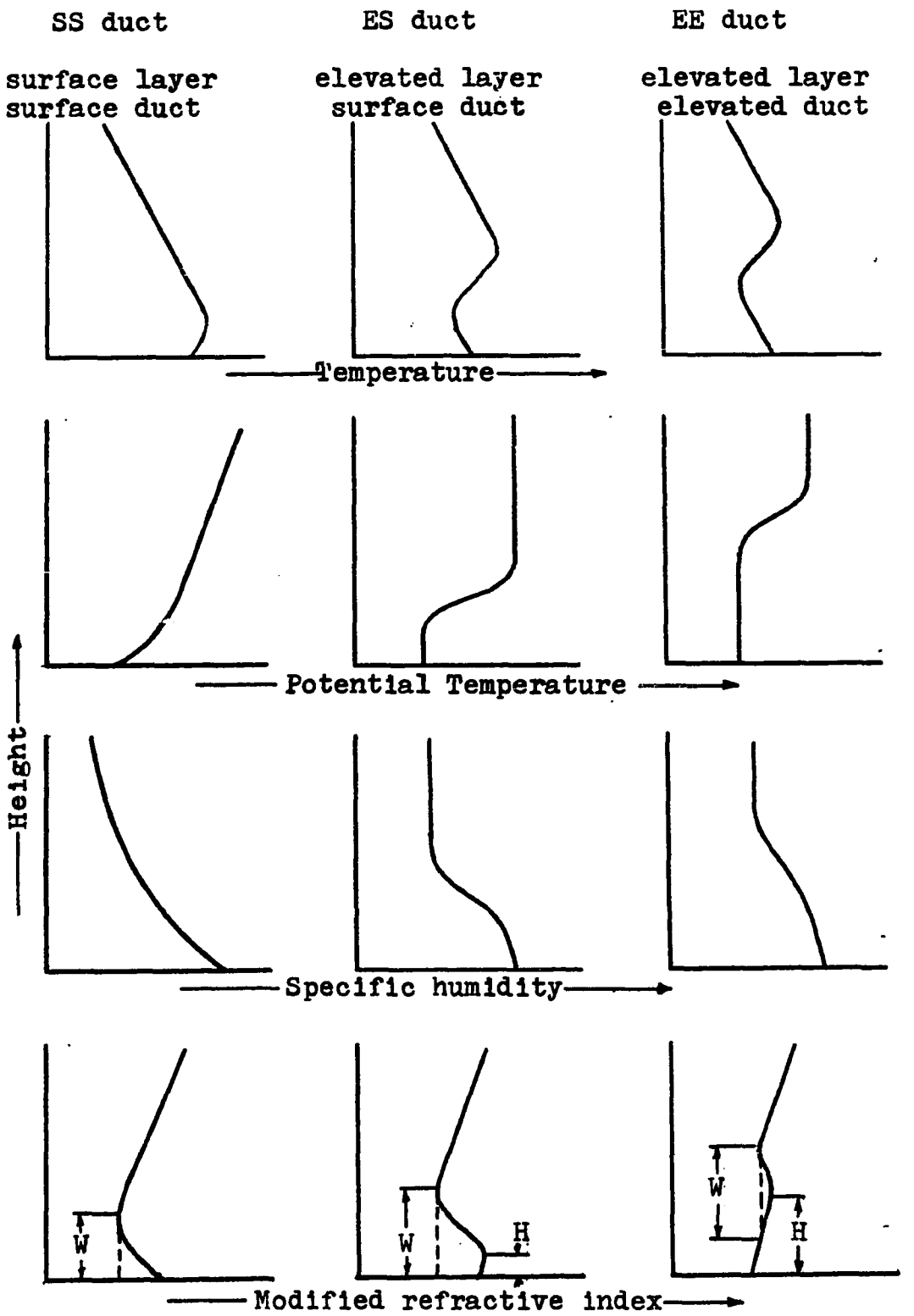

Figure 1.2. Types of radio ducts.

waveguide axis. It is possible, however, for a single conductive plate to act as a waveguide provided that it can constrain a wave launched over it to remain in contact with the surface. In surface microwave guides, a dielectric coating or corrugated structure facilitates the desired guiding function; in the troposphere, any guiding action depends upon the occurrence of a negative gradient of refractive index and one which is pronounced enough so that an upward-going wave will eventually be refracted downward. In elevated ducts, it is not necessary that a conductive wall be present.

There are two possible approaches to the analysis of modes in tropospheric waveguides. In the first and most frequently employed technique in the past, the phase integral approach (7, pp. 116-118), each component wave of the modes is made to satisfy the condition that upon complete traversal of the space between the guide walls or between the lower boundary of the guide and some to-be-determined height in the medium the total change in phase is some multiple of 2π radians. This method is extended to the case of a lossy medium by allowing complex values of phase, with the result that numerical solutions require the use of contour integration. The extension of the method was a contribution of Eckersley and Millington, op. cit. The method is also capable of dealing with the problem of diffraction around the

earth and the interested reader is referred to Budden for additional information.

The phase integral approach just sketched is essentially an application of ray theory to radio propagation and inherently is thus unable to account for the relatively strong fields outside ducts; furthermore, contour integration is not readily done numerically when the refractive index profile is not representable in terms of some simple functions. The full-wave solution appears to have the capability of surmounting the limitations of the previous method in the general case where the profile is best described by straight-line segments and the lower boundary is not plane. The full-wave solution arises from the use of the differential equation to describe the field inside the radio duct. To-date, it has been used by Wait and Spies(12) and Chang(13) in idealized mode problems.

SURFACE ROUGHNESS EFFECTS

Some of the motivation for studying the effects of surface roughness on tropospheric waveguides is due to the work which this writer did for his master's thesis on the subject of depolarization of electromagnetic waves by rough conducting surfaces. Terrestrial line-of-sight microwave communication links and other radio systems which operate near the earth's surface are susceptible to the effects of surface roughness. A search of the available literature revealed that previous investigators always assumed that the earth could be considered a smooth perfect conductor, even at wavelengths in which the roughness structure of the ground or sea was large in comparison with a wavelength. The assumption will often be acceptable at long wavelengths since the complex dielectric constant $\varepsilon_r - j\sigma/\omega\varepsilon_o$ will then have a large imaginary part. In this chapter, we will propose a method for including surface properties in the formulation of the waveguide-mode problem in surface-based tropospheric ducts.

The assumption of a perfectly conductive earth is equivalent to one of the following conditions, depending upon the polarization of the incident wave:

$$R_v = -1 \quad \text{or} \quad R_h = 1 \tag{2.1}$$

where R is the Fresnel reflection coefficient and the subscripts "v" and "h" stand for vertical and horizontal polarization, respectively. In the "full-wave" solution, to be discussed in the next chapter, equation (2.1) is equivalent to forcing one of the following conditions at z = 0:

$$f(z) = 0 \quad \text{(horizontal polarization)}$$

$$df/dz = 0 \quad \text{(vertical polarization)}$$

where f(z) refers to the electric field for horizontal polarization and to the magnetic field for vertical polarization. Approximating the reflection coefficient by +1 or -1 holds for a wide range of grazing angles and materials, as can be seen in Figures 2.1 and 2.2. This is especially true at low frequencies, corresponding to long wavelengths. This is indicated by the large values of $X = 60\sigma\lambda = \sigma/\omega\varepsilon_o$ on the two figures. It is the dependence of the Fresnel reflection coefficient upon the electrical constants of surfaces which will be exploited in the approach to be presented shortly. First, we will look at some of the simplifying assumptions employed in the method.

In a representative waveguide in the troposphere, the elevation angles of the wave normals are less than a degree; for soil and water, the magnitudes of the reflection coefficients are nearly equal to unity for near-grazing angles of

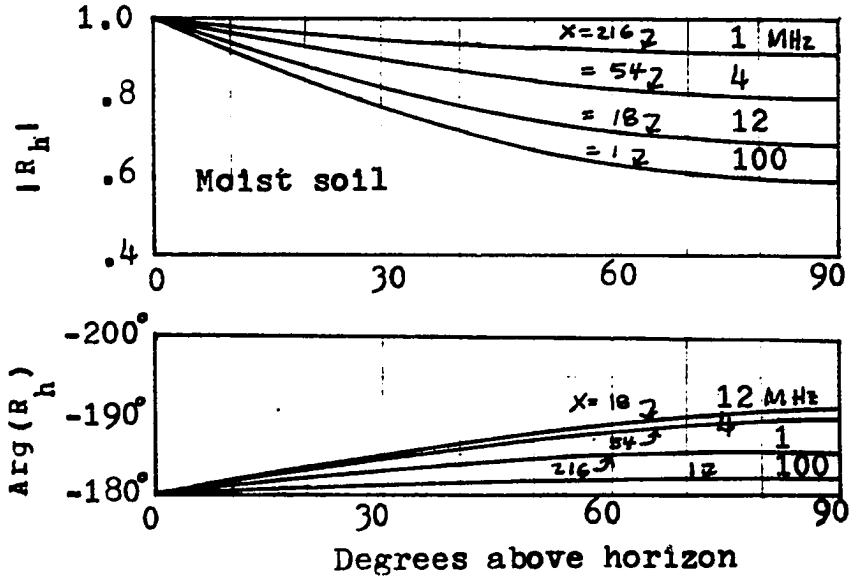

Figure 2.1. Magnitude and phase of Fresnel reflection coefficient for moist soil. Horizontal polarization.

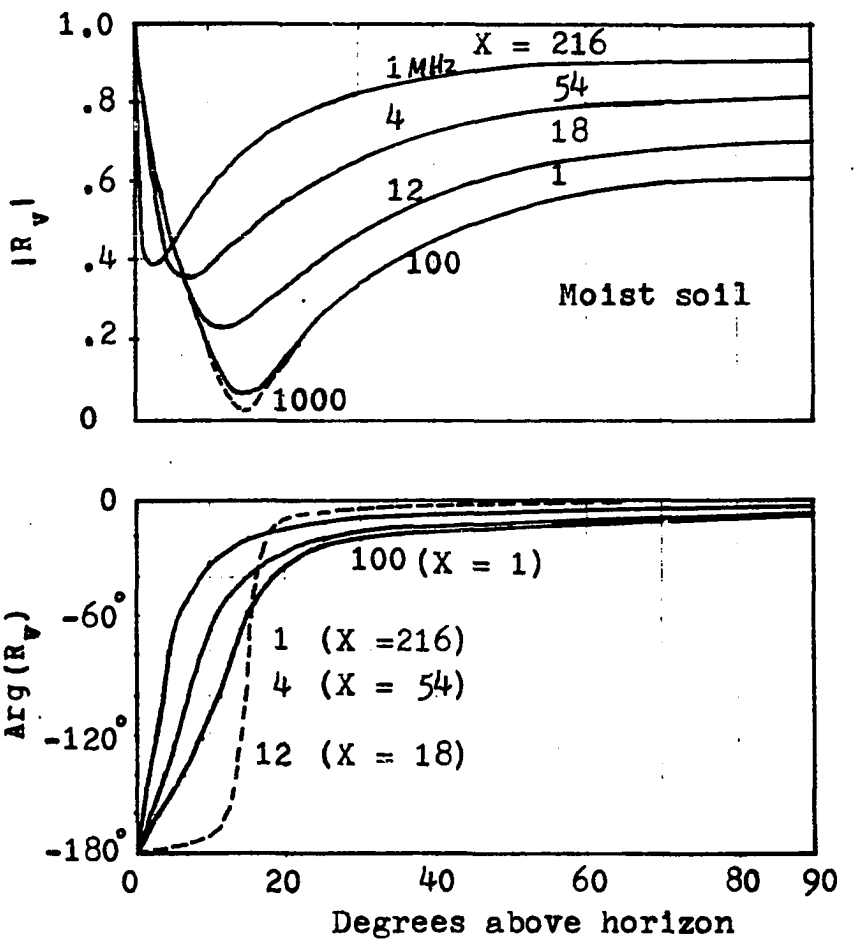

Figure 2.2. Magnitude and phase of Fresnel reflection coefficient for moist soil. Vertical polarization.

incidence. Such is not the case with ionospheric waveguides where the mode angles can be several degrees above the horizontal. Accordingly, the principal determining factor of the ability of the ground to reflect an incident wave is its roughness profile: the rougher the profile, the less energy is reflected in the specular direction.

For an estimate of the value of the angle of incidence which is to be used in calculating the equivalent surface constants, we will look at the ideal case when the lower boundary of the guide has perfect conductivity. For a given refractive index profile, we can solve for the directions of the wave normals for each mode. It is enough to consider only the first mode in a given case since this gives the lowest value of the angle of incidence θ. The angle θ is the angle between the wave normal and the vertical direction and is, in general, a complex quantity. In the case of tropospheric waveguides in which the lower boundary is not perfectly conductive, the mode angle will move away from the horizontal direction. We will not show this behavior here; the interested reader is referred to Budden (7, p. 143) in which plots of mode points on the complex θ-plane for the case of ionospheric modes are given for different ratios of conductivity to permittivity. The angles for the first few modes of a typical tropospheric waveguide are given in Table 2.1. The values are obtained from the expression

$$\sin^3\theta = 1.5\ K_1(m - 3/4), \quad m = 1, 2, \ldots \qquad (2.2)$$

where K_1 is the lapse rate (m^{-1}) and m is the mode order. This is the approximate mode equation for a guide with perfectly conducting walls.

From the numbers given in Table 2.1 or when equation (2.2) is solved, it can be seen that the lowest-order mode (m = 1) has the angle of 3.35 milliradians above the horizontal for the TM case, given a lapse rate of 10^{-7} per meter and a wavelength of 1 meter. Since the angle increases with lapse rate, this value represents a lower limit.

Table 2.1. Elevation angles of the first three modes in a duct over a perfect conductor. Refractive index profile is linear.

Mode order	Elevation angle (millirad)
1	3.35
2	5.72
3	6.96

Equivalent surface. The practical value of waveguide mode propagation theory can be enhanced considerably if it can be employed in those instances in which the lower boundary between the atmosphere and the earth is rough. One approach which might be used is that described by Senior (14). His method uses an imperfectly conducting plane surface to replace a rough contour, the conductivity of the equivalent surface being a function of the roughness and the electromagnetic properties of the original surface. The equivalence is established by forcing the boundary conditions for the two surfaces to be identical. Having defined the electrical parameters of the equivalent surface, it is then possible to set up the waveguide-mode problem for the case in which the lower boundary of a duct is is a plane, imperfect conductor. The presence of an imperfect conductor necessitates the use of an impedance boundary condition (11,15). This condition expresses a relationship between the tangential components of the electric and magnetic fields at an interface between a dielectric medium and an imperfect conductor.

We will not, however, use Senior's method for this present work; instead, we will introduce a less sophisticated characterization of the effects of a rough contour. The method to be used does not depend upon restrictive conditions with respect to the rough surface being considered; on the contrary, irrespective of the degree of roughness, if F_{rs} is

specified, then an equivalent surface can always be found. As presented below, the technique merely accounts for one aspect of rough-surface scattering, namely that of the reduction in the intensity of the field in the specular direction relative to the mean plane of the rough surface. There are other processes which are generally involved in rough-surface scattering, including shadowing, depolarization, and multiple scattering. All of these would exert some degree of influence upon the reflected field. Accordingly, it should be emphasized that the use of the reflection factor F_{rs} is appropriate only for the component of the scattered field which has the same polarization as the incident field which produced it.

Consider the simplified approximation of a rough contour by means of an array of flat facets tangent to the original rough surface. Figure 2.4 shows how a rough contour might be approximated by short straight-line segments which are locally tangent to the rough contour. For the two-dimensional case, these lines would be replaced with rectangular facets or some other appropriate two-dimensional shapes. The linear dimensions and angular orientations of these elementary reflectors would generally be randomly distributed. In this representation of the rough contour, we note that there has to be a trade-off between the accuracy of the approximation of the contour with the flat facets and the specular charac-

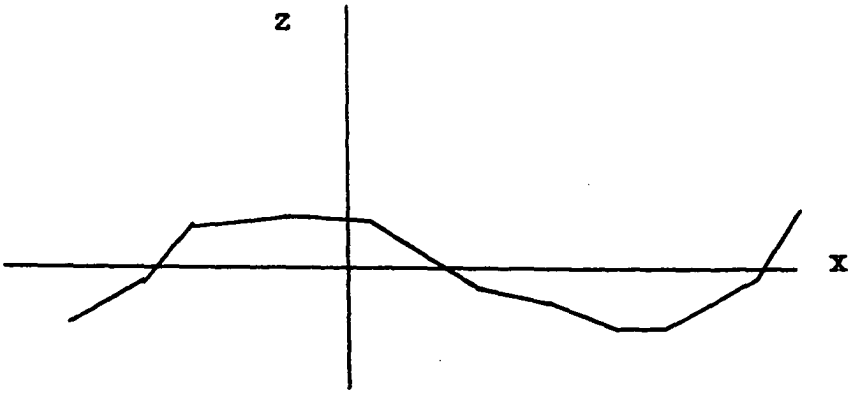

Figure 2.4. Approximation of an irregular contour using straight-line segments. x scale is compressed.

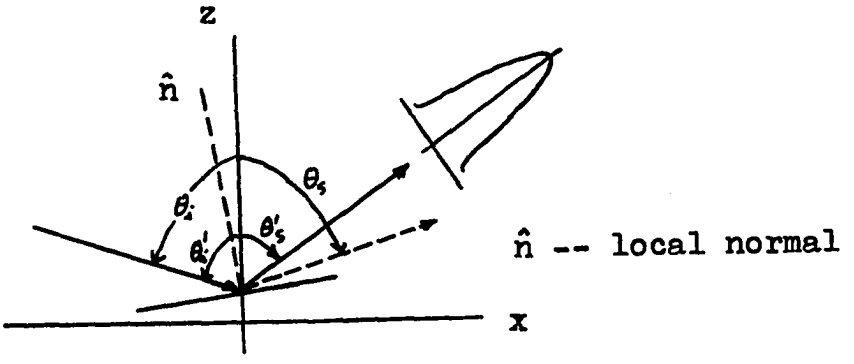

Figure 2.5. Local scattering geometry and sketch of scattering pattern from plane strip.

ter of the fields scattered from the elementary scatterers. With this property, reflection from each facet will be essentially specular; wave reflection theory for rectangular plates with finite area(20) will show that the scattered field will have a pattern described by the product of

$$(\sin x)/x \qquad (2.3)$$

where $x = \pi a \sin\theta/\lambda$
a = length of a side of the rectangle
θ = angle of incidence
λ = wavelength

Figure 2.5 shows how a single facet might reflect an incident wave. Also shown is the assumed sinx/x pattern of the reflected field. This shape becomes sharper as the angle of incidence increases to glancing and the linear dimensions are increased. Thus to a first order approximation, the far field will be due to specular contributions from each area, with those facets lying near the horizontal providing the major contribution. The implication of the preceding argument is that the rough contour scatters with a reduced area, resulting in a far field which will be attenuated.

Calculation of equivalent surface constants. Let the far field in the rough-surface case be E' due to an incident field E_i. Corresponding to these quantities we define an effective reflection coefficient R':

$$R' = E'/E_i \tag{2.4}$$

Next we introduce the rough-surface reflection factor F_{rs}, which is defined as

$$F_{rs} = R'/R \tag{2.5}$$

where R is the Fresnel reflection coefficient of a smooth surface, R' that for the rough contour.

The reflection factor F_{rs} is a tensor function of the roughness and electrical parameters of the surface, the angle of incidence, and the wavelength. From this point, however, we will not be concerned with obtaining a mathematical expression for F_{rs} since this is another whole area of investigation by itself; Senior's two articles (14,15) could be useful starting points for such a study. Although F_{rs} is a tensor, we will employ the simplification that the scattered field is primarily due to the contributions of areas of the surface which have their planes oriented close to the horizontal so that it is reasonable to take F_{rs} to be a scalar quantity. In the limit, as the rms roughness height goes to zero and/or as the correlation length increases, corresponding to a smooth surface, F_{rs} will tend toward unity since then the whole surface will be contributing to the far

field. In what follows, F_{rs} will be some number less than or equal to unity, depending upon whether the rough surface is more or less effective in reducing the scattered field. The Fresnel reflection coefficient of a plane surface illuminated by a wave incident at the grazing angle ϕ, and having the constants ε_r and σ is

$$R = \frac{(\varepsilon_r - jX)\sin\phi - (\varepsilon_r - jX - \cos^2\phi)^{1/2}}{(\varepsilon_r - jX)\sin\phi + (\varepsilon_r - jX - \cos^2\phi)^{1/2}} \qquad (2.6)$$

where $X = 60\sigma\lambda$.

Now a rough contour, made up of the same material, will by our postulate, have an effective reflection coefficient

$$R' = -a - jb \qquad (2.7)$$

where a and b are real and $|R'| \leq 1$, and which could be related to the plane surface reflection coefficient R via the reflection factor F_{rs} as given in equation (2.6). Using the expression for the Fresnel reflection coefficient, we can derive an inversion equation for finding the constants of the equivalent surface. For the equivalent surface, we have the equivalent or effective reflection coefficient R'

$$R' = \frac{c'\sin\phi - (c' - \cos^2\phi)^{1/2}}{c'\sin\phi + (c' - \cos^2\phi)^{1/2}} \qquad (2.9)$$

where $c' = \varepsilon_r' - j\sigma'/\omega\varepsilon$. This is equation (2.4) written for a material with the complex dielectric constant c'. By a simple algebraic manipulation of the preceding equation, we can get an expression for the complex dielectric constant c' in terms of R' and ø:

$$R'(c'\sin\phi - (c' - \cos^2\phi)^{1/2} = c'\sin\phi - (c' - \cos^2\phi)^{1/2} \tag{2.10}$$

where again $c' = \varepsilon_r' - j\sigma'/\omega\varepsilon$.

Rearranging to place the terms involving the square root on one side of the equation, we have

$$c'\sin\phi(R' - 1) = -(c' - \cos^2\phi)^{1/2}(R' + 1) \tag{2.11}$$

After squaring and performing additional manipulations, we finally get the second-order equation in the complex dielectric constant c':

$$(c'\sin\phi)^2(R' - 1)^2 = (c' - \cos^2\phi)(R' + 1)^2 \tag{2.12}$$

This can be solved to yield

$$c' = \frac{T \pm (T^2 - 4ST\sin^2\phi\cos^2\phi)^{1/2}}{2S\sin^2\phi} \tag{2.13}$$

where $S = (R' - 1)^2$

$T = (R' + 1)^2$

Of the two possible answers coming out of this expression, we will pick the one which gives relatively large permittivity and conductivity since an impedance condition in which the equivalent constants will be used will require that the refractive index of a material be much greater in magnitude than unity. The other equivalent constant is nearly equal to unity. It may be pointed out that for this latter case where the equivalent constant is nearly that of air, the wave will penetrate into the lower medium via refraction at a low grazing angle. In the case of the equivalent constant which is large in magnitude, the angle of refraction in the lower medium will approach 90 degrees and the low value of the reflection factor for this equivalent plane surface will be a consequence of conduction losses.

Figures 2.6 to 2.8 show how the equivalent surface constants of different materials vary as a function of wavelength, F_{rs}, and the angle of incidence. For all of these materials, as the surface becomes less effective in reflecting an incident wave, the equivalent permittivity and conductivity increase.

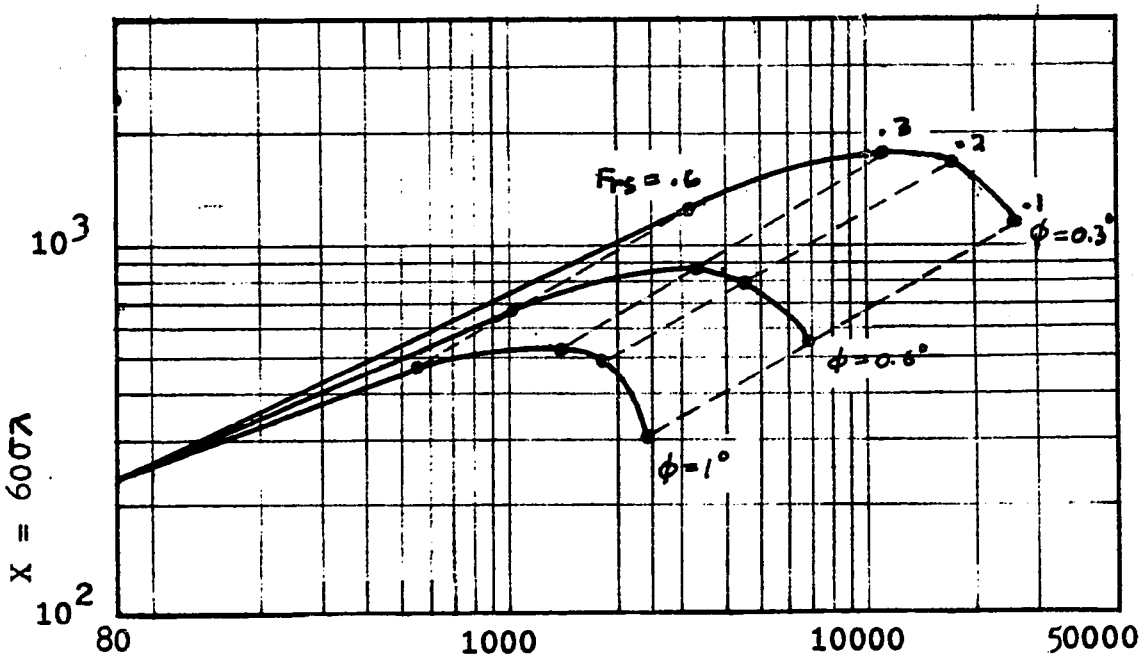

(a) Sea water

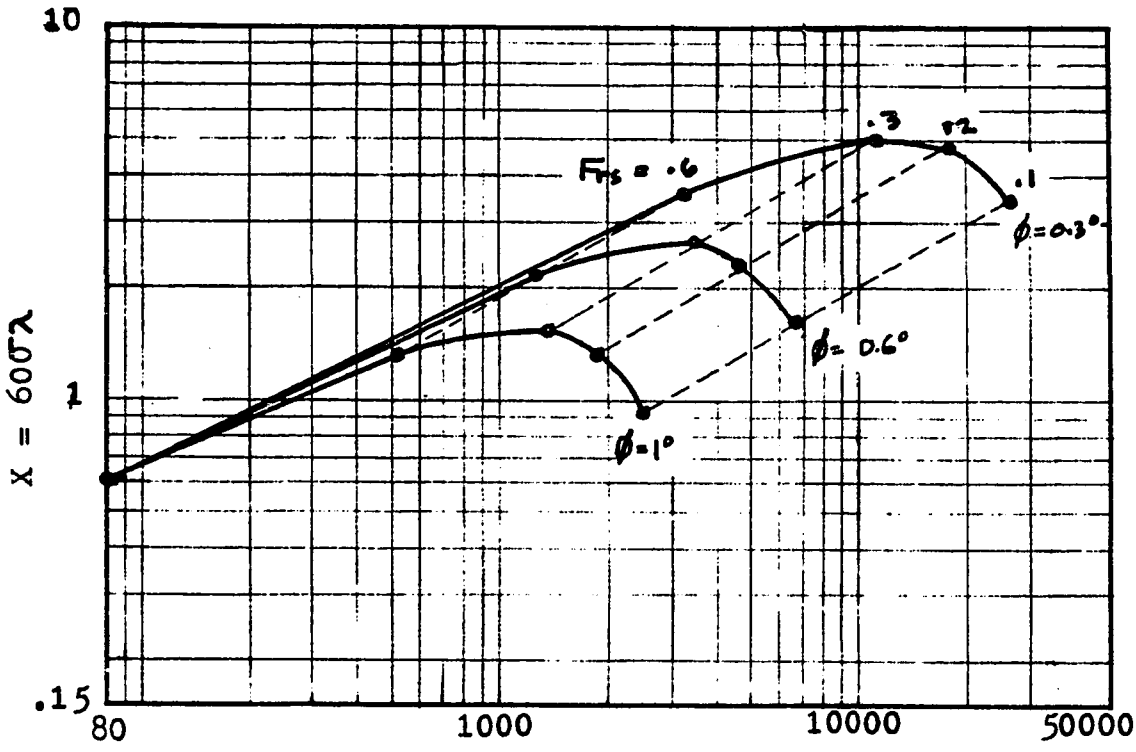

Relative permittivity

(b) Fresh water

Figure 2.6. Equivalent surface constants for rough sea and fresh water surfaces.

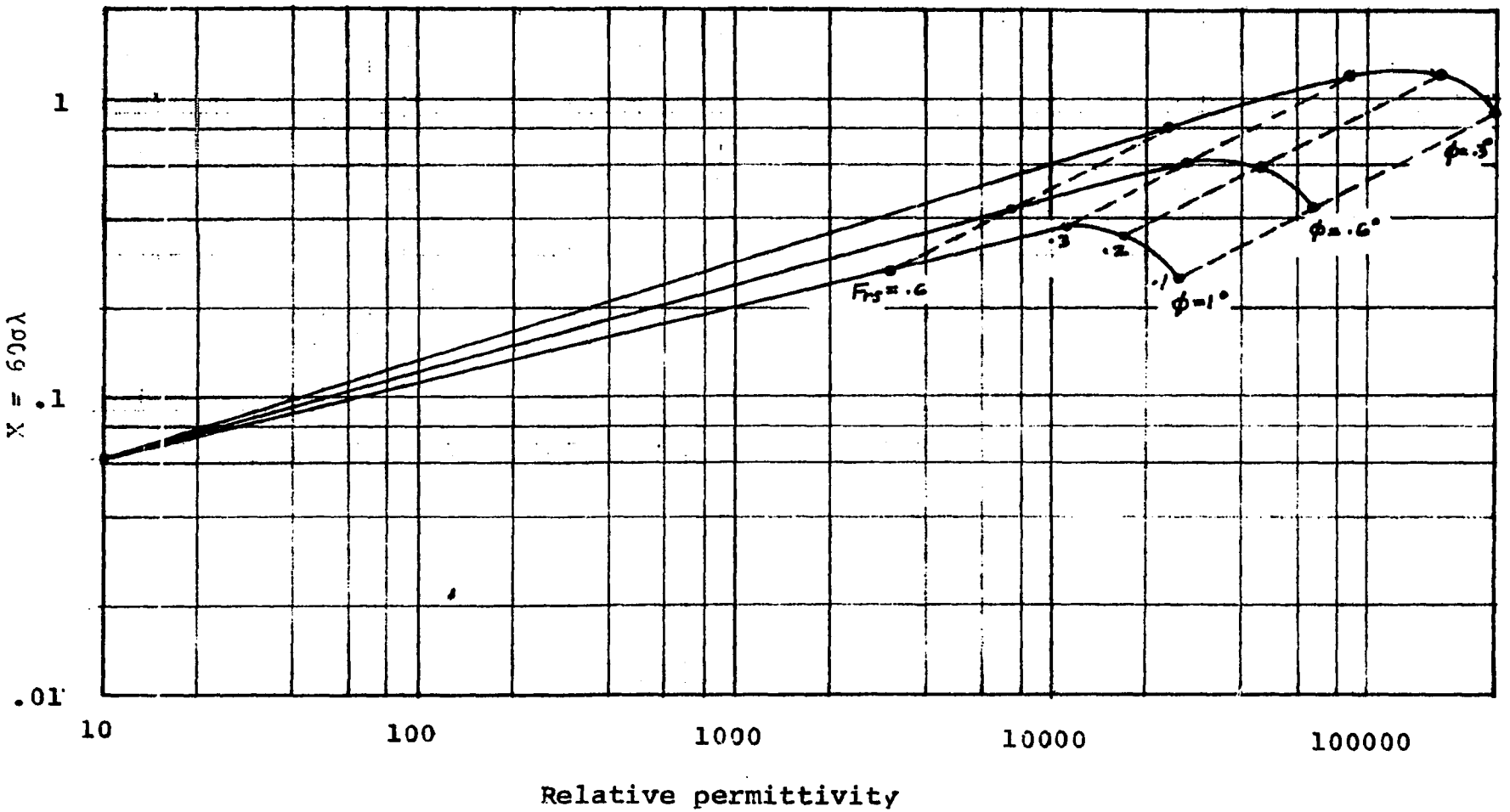

Figure 2.6. Equivalent surface constants for moist soil at different values of F_{rs}. Parameter for each curve is Ø in degrees.

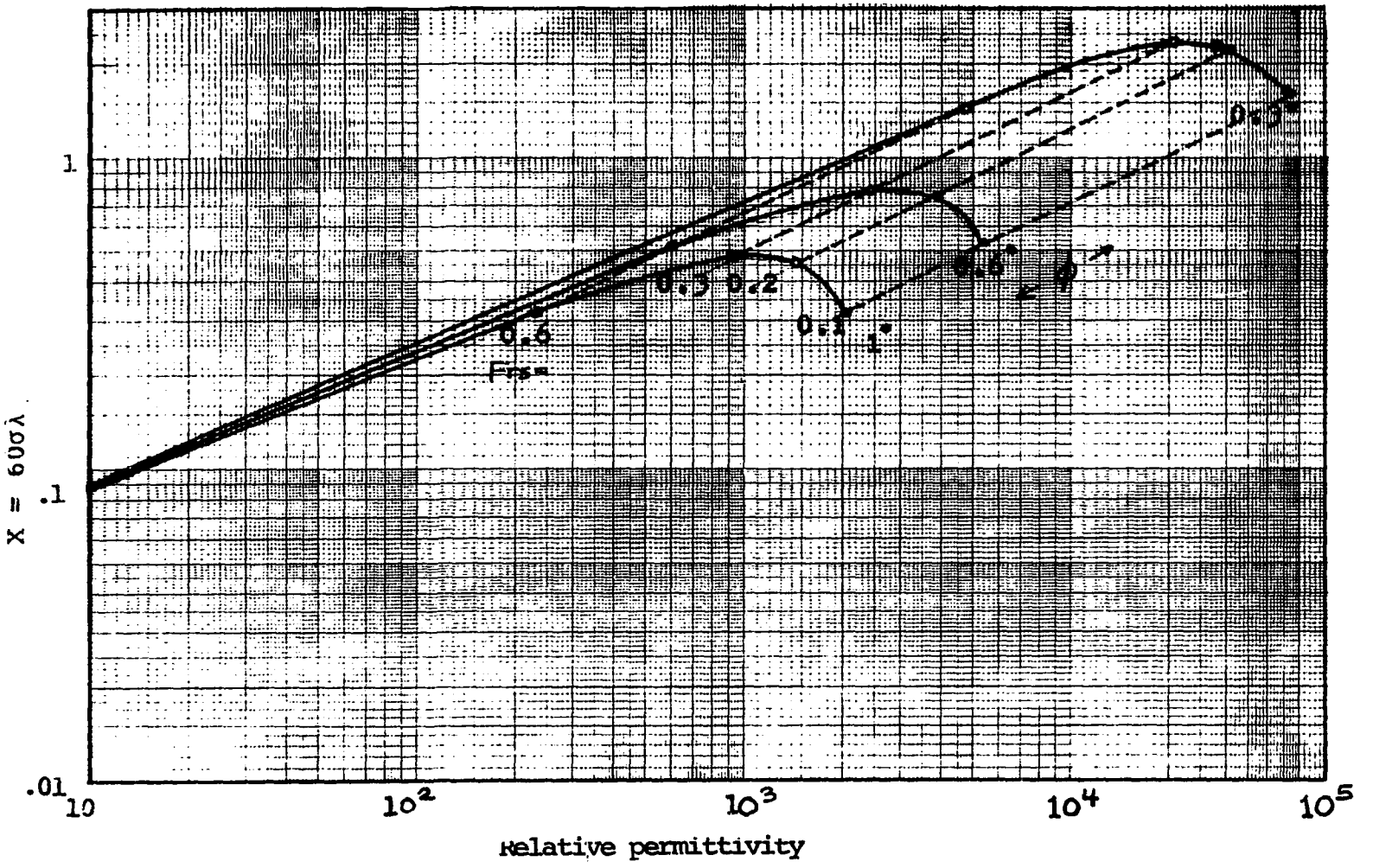

Figure 2.7. Equivalent surface constants for sea water at different values of F_{rs}. Parameter for each curve is Ø in degrees.

WAVEGUIDE-MODE ANALYSIS

General. In order to demonstrate the role of surface roughness on the properties of tropospheric waveguides, through the the artifice of an equivalent complex dielectric constant with finite conductivity, we will examine two simple profiles: linear and bilinear, as shown in Figure 3.1 below.

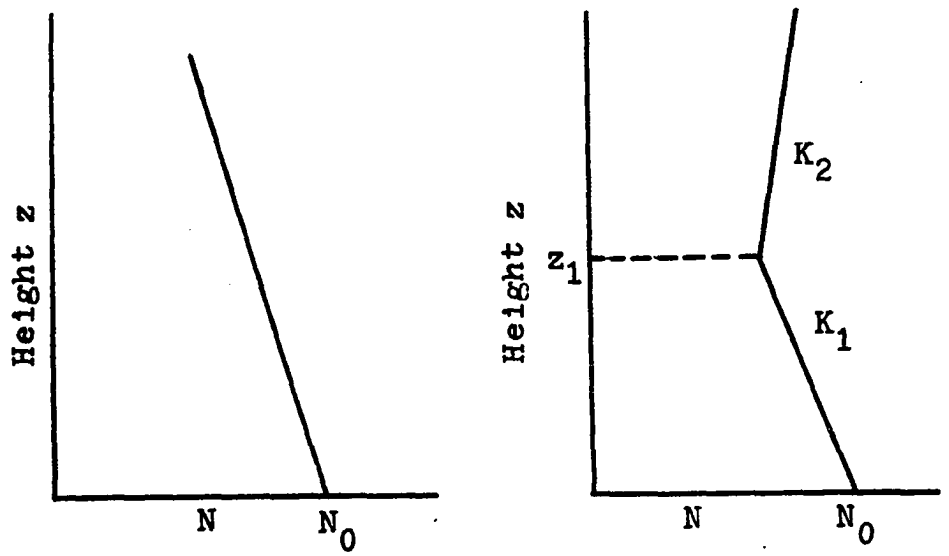

(a) Linear (b) Bilinear

Figure 3.1. Simple linearized refractive index profiles.

Mode attenuation and phase velocity as functions of wavelength, lapse rate, duct height and surface roughness constants will be calculated. For comparison, data on ideal waveguides and linear M-profiles and smooth-earth diffraction

parameters will also be cited. The approach uses a linearly-segmented representation of actual profiles. By using this segmentation of the profile, there will be no unwanted reflections which would otherwise occur at step discontinuities in the refractive index.

Basic method. Consider a 2-dimensional waveguide in which a vertically polarized plane wave is obliquely incident. The refractive index profile in the medium inside the duct is subdivided into layers, inside each of which the M-profile is a linear function of height z. Since very small changes of refractive index are involved, in a given layer having lapse rate K_1 the square of refractive index can be approximated by

$$n^2(z) = 1 - 2K_1 z \qquad (3.1)$$

The field inside the guide can be expressed in the product form

$$F(x,z) = f(z)\ \exp(-jkCx) \qquad (3.2)$$

where $C = n\cos\phi$ = a constant by Snell's law
z = vertical height
x = distance along the direction of propagation
k = wave number

Note that the sinusoidal time dependence has been suppressed in equation (3.2). For a specified M-profile, the wave will be a solution of the second-order differential equation (7, p.181)

$$d^2f/dz^2 + k^2(n^2 - C_m^2)f = 0 \qquad (3.3)$$

where C_m is the eigenvalue corresponding to the m-th mode. This can be rewritten as

$$d^2f/dz^2 + (g(z) + \gamma)f = 0 \qquad (3.4)$$

where $g(z) = k^2n^2(z)$
$\gamma = -k^2C_m^2$

In a representative stratum (z_{j+1}, z_j), Eq.(3.4) becomes

$$d^2f/dz^2 + [B_j(z-z_j) + g(z_j) + \gamma]f = 0$$

where $B_j = [g(z_{j+1} - g(z_j)]/(z_{j+1} - z_j) = 2k^2K_j$, K_j being the lapse rate in the layer between z_{j+1} and z_j. By means of the transformation

$$\eta_j = -B_j(z - z_j + (g(z_j) + \gamma)/B_j). \qquad (3.6)$$

where B_j and K_j are as defined above, and $B' = B^{1/3}$, the differential equation (3.4) in turn becomes the Stokes equation(13)

$$d^2f/du^2 - uf = 0 \tag{3.7}$$

The general solution of equation (3.7) is (17, p.446)

$$f(z) = CAi(u) + DAi(u') \tag{3.8}$$

where $u = u \exp(-j2\pi/3)$ and $Ai(u)$ and $Ai(u')$ are the Airy integral functions which are entire on the complex u-plane.

The mode equation for a given profile is set up by using Eq. (3.8) in the impedance boundary condition at the ground ($z = 0$) and continuity conditions at interfaces between layers. The impedance boundary condition is in effect another way of expressing the relationship between the incident and reflected waves at the interface between two media, one of which is usually air and the other an imperfect conductor with electrical constants ε_r and σ. For vertical polarization we have the equation

$$df/dz + qf = 0 \tag{3.9}$$

where again $q = -jk/(\varepsilon_r - j\sigma/\omega\varepsilon)^{1/2}$. This equation can be derived following a procedure given in (11, p.21). The following are the mode conditions for the linear and bilinear profiles.

Using a physical argument, the condition that the solutions be bounded for very large heights requires that the second term of equation (3.8) be zero in the case where the refractive index has a negative gradient with height. Then the resultant solution for the linear case is

$$f(z) = PAi(u) \tag{3.10}$$

Consequently, when we substitute this solution into the boundary condition at $z = 0$, we obtain the mode equation

$$-B'Ai(u) + qAi(u) = 0 \tag{3.11}$$

where $q = -jk/(\varepsilon_r - j60\sigma\lambda)^{1/2}$

Bilinear profile with lapse rate K_1. For an improved approximation of an inversion layer as compared with a duct with a linear profile, examine a bilinear profile as shown in Figure 3.1(b). The profile is assumed to have a lapse rate K_1 over the interval $(0,z_1)$ and above z_1 the normal tropospheric gradient K_1 is assumed. In the duct with the

bilinear profile, there will be two layers for which solutions to Maxwell's equations can be written. As in the linear case, the solution $f_1(z)$ must satisfy the impedance boundary condition at $z = 0$. In addition, the solutions $f_1(z)$ and $f_2(z)$ and their normal derivatives are continuous across the interface at $z = z_1$. In each of these layers we have the following solutions to Stokes equation:

Layer 1: $0<z\leq z_1$.

$$f_1(z) = P_1 Ai(u_1) + Q_1 Ai(u_1') \tag{3.12}$$

$$n_1^2(z) = 1 - 2K_1 z \tag{3.13}$$

Layer 2: $z\geq z_1$.

$$f_2(z) = Q_2 Ai(u_2') \tag{3.14}$$

$$n_2^2(z) = 1 - 2K_1 z + 2K_2(z - z_1) \tag{3.15}$$

P_1, Q_1, and Q_2 are arbitrary constants and

$$u_1 = -B_1'[z + (1 - C_m^2)/(-2K_1)] \tag{3.16}$$

$$u_2 = -B_2'[z + (1 - C_m^2 - 2K_1 z_1)/2K_2] \tag{3.17}$$

$$B_1' = -(2k^2K_1)^{1/3} \tag{3.18}$$

$$B_2' = (2k^2K_2)^{1/3} \tag{3.19}$$

The complex variable u_{ij} denotes the quantity u_i defined for the i-th layer and evaluated at the height z_j. The eigenvalue C_m can be found by applying an impedance boundary condition at z = 0 and continuity conditions at $z = z_1$. Thus at the ground, we have the expression

$$P_1[-B_1'Ai'(u_{10}) + q\,Ai(u_{10})] +$$
$$Q_1[-B_1'\exp(-j2\pi/3)\,Ai'(u_{10}) + qAi(u_{10}')] = 0$$

where u_{10} and u_{10}' are u_1 and u_1', respectively, evaluated at z = 0.

At $z = z_1$, $f_1 = f_2$ and $df_1/dz = df_2/dz$:

$$P_1Ai(u_{11}) + Q_1Ai(u_{11}') = Q_2Ai(u_{21}') \qquad (3.21)$$

and

$$-P_1B_1'Ai'(u_{11}) - Q_1B_1'Ai'(u_{11}')\exp(-j2\pi/3)$$
$$= -Q_2B_2'Ai(u_{21}')\exp(-j2\pi/3) \qquad (3.22)$$

Equations (3.20) to (3.22) can be solved to give the mode equation.

$$D = GU + TV \qquad (3.23)$$

where $G = IAi(u_{11}) + B_1'Ai'(u_{11}')Y\exp(-j2\pi/3)$

$$T = IAi(u_{11}) + YB'Ai'(u_{11})$$

$$U = -B_1' Ai'(u_{10}) + qAi(u_{10})$$

$$V = qAi(u_{10}') - B_1' Ai'(u_{10}') \exp(-j2\pi/3)$$

$$I = -B_2' Ai'(u_{21}') \exp(-j2\pi/3)$$

$$Y = Ai(u_{21}')$$

For a more general profile subdivided into J segments, there will be (J - 1) arbitrary constants P_j and Q_j. There will also be (2J - 1) conditions: the impedance boundary condition at the ground and two continuity conditions at each of the boundaries between layers.

NUMERICAL METHOD

Having arrived at a possible representation of a rough surface using the concept of an equivalent surface with modified complex dielectric constants, we now proceed to describe the important aspects of the numerical solution of the waveguide-mode equation of the preceding chapter. The numerical solution consists of three parts: (1) the statement of the mode equation(s), (2) the development of the necessary routines for evaluating the Airy integral functions Ai(u) and Ai'(u) and (3) the development of a root-finding routine for solving the mode equation.

Airy integrals. The successful solution of the waveguide-mode problem even for the comparatively simple profiles considered here depends to a large extent upon the accuracy and precision of the Airy integral function routines. The Airy integral functions which are the solutions of the second order differential equation called Stokes equation can be expressed in the ascending power series form of the complex argument u and u' (18,p.446),

$$Ai(u) = c_1 f - c_2 g \qquad (4.1)$$

where $f = 1 + u^3/3! + 1\cdot 4u^6/6! + 1\cdot 4\cdot 7u^9/9! + \ldots$

$g = u + 2u^4/4! + 2\cdot 5u^7/7! + 2\cdot 5\cdot 8u^{10}/10! + \ldots$

$c_1 = 3^{-2/3}\Gamma(2/3)$

$c_2 = 3^{-1/3}\Gamma(1/3)$

$u' = u\exp(-j2\pi/3)$

By differentiating with respect to the complex argument u_{ij}, the series expansion for the first derivative of the Airy integral function can also be found. Use will also be made of the identity

$$Ai''(u) = uAi(u) \tag{4.2}$$

In the foregoing expression, the primes indicate differentiation with respect to the argument of the Airy function. The series f and g above can be shown to be convergent over the region of interest in this work. Due to the limitations of the procedure used for evaluating the Airy integral functions, the waveguide mode problems which can be solved by the present method are those for which the modulus of any argument does not exceed 9. The first three modes of the ideal waveguide problem, for which the lower boundary is assumed to be a perfect conductor, correspond to zeros of the Airy integral function and its first derivative which lie within this region. We are primarily interested in the lowest three or four modes since these are the least attenuated of the waveguide modes.

The evaluation of the Airy integral functions can best be done be rewriting the series in factored or nested form which permits a high number of significant digits to be retained following a large number of arithmetic operations associated with the evaluation of the series. Accordingly we have for a series of k terms the following expression:

$$f = 1 + \frac{u^3}{3\cdot 2}\left(1 + \frac{u^3}{6\cdot 5}\left(\ldots + \frac{u^3}{3k(3k-1)}\right)\right)\ldots) \tag{4.3}$$

$$g = u\left(1 + \frac{u^3}{3\cdot 4}\left(1 + \frac{u^3}{6\cdot 7}\left(\ldots + \frac{u^3}{3k(3k+1)}\right)\right)\ldots\right) \tag{4.4}$$

The essential advantage in using the factored form is that the operations resulting in the smallest numbers are evaluated first so that for the power series we are concerned with the sum

$$1 + u^3/p(k) \tag{4.5}$$

where $p(k) = 3k(3k - 1)$ or $3k(3k + 1)$

for which the second term is approximately 10^{-2}. The method is especially important when the modulus of the complex argument u is large, such as when $|u|$ is about 9. In this case, f and g are relatively large quantities, of the order of 10^6 or so, such that after evaluating the Airy integral function,

the maximum number of digits that can be expected to be meaningful could be not much more than 6 to 8 so that the use of extended precision arithmetic (16-byte complex representation) on the IBM 360 was absolutely justified.

In order to determine the number of terms needed in a given evaluation of the Airy integral functions, it was decided to carry out the evaluation of the integrals for different numbers of terms in the series expansion. This was done by varying the phase angle of the complex argument and evaluating the truncated series until no further improvement in the sum was seen. The result for arguments with different magnitudes is given in Table 4.1 and essentially indicate that the logarithm of the number of terms required corresponds to the modulus of the argument u.

Table 4.1. Number of terms required for power-series expansion of Airy integral functions.

mod (z)	Number of terms
2	12
4	18
5	22
6	28
7	32
8	34
9	42

Newton-Raphson method. For a root-finding technique, it was decided to use the Newton-Raphson procedure since it can work equally well with expressions involving complex as well as real arguments. The method is defined for the complex equation

$$F(u) = g(u) + jh(u) \tag{4.6}$$

where $F(u)$ is an analytic function of the complex variable $u = x + jy$ and $g(u)$ and $h(u)$ are real for all u. The Newton-Raphson method is defined

$$u_{n+1} = u_n - F(u_n)/F'(u_n) \tag{4.7}$$

where u_n is an estimate of the desired solution u_{10}. When $F(u_n) = 0$ when $F'(u_n) = 0$, then

$$u_n = u_{n+1} \tag{4.8}$$

For starting solutions u, the real zeros of the Airy integral function or its first derivative are used The mode equations are not directly expressed as functions of the desired eigenvalue; instead, they are solved for in terms of the argument of the Airy integral function v_{10}. After finding u_{10}, it is a simple procedure to calculate the eigenvalue

$$C_m = n\cos\phi_m = (1 + 2u_{10}K_1/B') \qquad (4.9)$$

The mode equation is expressible in terms of the argument u since all the other arguments can be expressed in terms of it. The flow chart for the Newton-Raphson root-finding routine is shown in Figure 4.1. Briefly, it has the expressions for the mode equation D and its first derivative with respect to the argument u and subroutines for evaluating the Airy functions Ai(u) and Ai'(u). A routine for assigning the number of terms to a series expansion for an Airy function depending upon the modulus of the argument u is also included. The input data are

Z1	duct depth, W
RL1	lapse rate K
Z	trial solution of mode equation
RL	relative permittivity
RX	$X = 600\sigma\lambda$
DERR	error limit

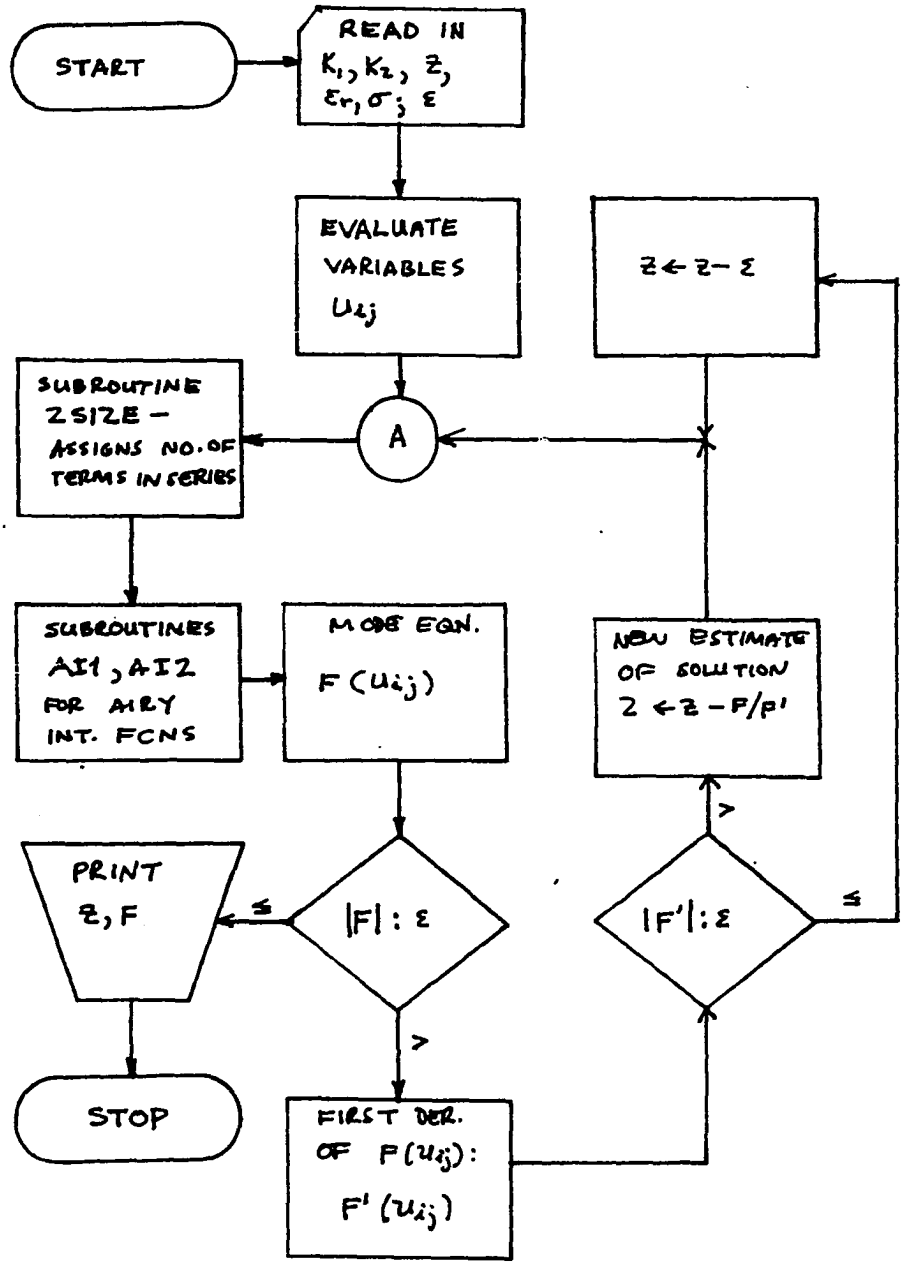

Figure 4.1: Flow chart for Newton-Raphson routine for solving waveguide mode equation.

NUMERICAL RESULTS

Calculations were made for the two simple profiles described in chapter 3. For a reference against which the properties of the modes in ducts over rough surfaces can be measured, the ideal case in which the earth is assumed to be a perfect conductor was investigated. For the case of a duct having a linear refractive index profile, the mode properties are given in the literature. It was primarily to test the correctness of the equations used in the analysis that the ideal cases were studied. The data can be divided into those applicable to ducts having smooth lower walls and those for ducts underlain by rough contours. The former category by themselves constitute an important group of problems since previous treatments of surface-based ducts employed the severe simplification that the ground or water surface can be represented by a perfect conductor. The second set of results dealing with the solution of the waveguide-mode problem for roughened contours represent a new method of accounting for roughness effects. In a duct with a bilinear profile, attenuation rates of the various modes can be readily obtained by simply using $q = 0$. For vertical polarization, this is equivalent to the mode equation $df/dz = 0$.

Figure 5.1 shows how the lapse rate in a duct with a linear profile of refractive index affects the rate of atten-

uation of waveguide modes. The curve shown for each material applies to the next two modes (at least), since the numerical results at corresponding lapse rates were close in value to each other. Next, figures 5.2 and 5.3 show how attenuation is changed when the lower boundary of the duct becomes rough. The data shown are for reflection factors (F_{rs}) of .1, .2, .3, .6, and 1.0 with lapse rate (K_1) of 10^{-7} per meter and a wavelength of 1 meter. Note that to find these attenuation rates the equivalent surface constants are different for the three modes and can be taken from figure 2.4 or 2.5. The next two figures, 5.4 and 5.5, show how the attenuation rate varies with lapse rate for smooth sea and moist soil, respectively. The lapse rates used were 10^{-8}, $5x10^{-8}$, and 10^{-7} per meter. The independent variable for the figures is duct depth W. Figure 5.6 indicates the manner in which surface roughness modifies the attenuation curves given in figure 5.4 for sea water. The next two figures, 5.7 and 5.8, show how the attenuation rate varies with duct depth W. Three curves are shown for the first three modes in the bilinear duct. The effects of roughness in wave propagation inside a bilinear duct is indicated in figures 5.9 and 5.10 for sea water and moist soil at $F_{rs} = 0.3$. Finally, the last two figures (figures 5.11 and 5.12) portray the effect of varying the wavelength for a given bilinear duct. Three duct depths z = 100, 150, and 200 meters are used as parameters. Due to

the limitation in computation time, a more representative collection of results is not possible; however, the present data should serve to demonstrate the importance of surface roughness and finite conductivity on radiowave propagation along the earth's surface by the ducting process.

From the definition of the variable u,

$$u_m = -B_1'[z + (1 - C_m^2)/(-2K_1)] \qquad (5.1)$$

we can determine the eigenvalue C_m once the zero of the mode equation has been found. The attenuation rate a of each mode is calculated using the expression

$$a_m = -kIm(C_m) \times 8686 \text{ dB/km} \qquad (5.2)$$

where again k is the wave number at z= 0, $C_m = n\cos\phi_m$.

The effective phase velocity of the electromagnetic wave inside the duct is reduced somewhat, as it turned out, by about a few parts in 10^3 or 10^4 at the most. Accordingly, only the attenuation rates of the modes are presented as these depend upon the tropospheric conditions, polarization, wavelength, surface material and surface roughness.

In starting the numerical solution of the mode equations for the linear and bilinear cases, the real zeros of the Airy integral functions Ai(u) and Ai'(u) were appropriate since

the zeros are the solutions for the ideal duct whose lower boundary is a perfect conductor. The choice of starting points for the initial estimate of the solution of the mode equation for the practical situation in which the earth is not perfectly conductive turns out to be dependent upon the relative magnitude of the terms in the mode equation. Consider the mode equation for the duct with a linear profile:

$$df/dz + qf = 0 \text{ at } z = 0 \tag{5.3}$$

In terms of the Airy integral function, we have the equivalent expression

$$(-B')df/du + qf = 0 \tag{5.4}$$

where typically B' is of the order of 10^{-2} or less so that the first term is about two orders of magnitude smaller than the term in f. Consequently, when q is large, the desired solution of the mode equation is essentially determined by the zero of Ai(u); otherwise, Ai'(u) determines the solution. For the cases examined in the numerical calculations, there are examples of both types of solutions.

Some of the approximations made in finding the waveguide modes of the radio duct will next be given. Recall that the factor q in the mode equation of the linear profile case is a

function of the surface impedance of the ground. In all the cases involving smooth surfaces, solutions were sought under the assumption that surface impedance presented by the ground to an incident wave is to a good approximation the same as its characteristic impedance. A more accurate representation of the ground's surface impedance uses the following modification:

$$Z = \eta [1 - (\gamma_0^2 \sin^2\theta)/\gamma_1^2]$$

where η = characteristic impedance of the ground

$$\gamma_0^2 = -\epsilon\mu\omega^2$$

$$\gamma_1^2 = j\omega\mu\sigma_1 - \epsilon_1\mu\omega^2$$

It turns out however that the dependence upon the angle of incidence is a second-order effect since the cosine of a small angle, approximately .01 radian, is involved. This is especially true when the ratio γ_0/γ_1 is small, such as for sea water. For the case of dry soil, which has a relative permittivity of 4 and a conductivity of 10^{-3} mhos per meter, the correction would have to be made if a high degree of accuracy is desired. On the other hand, in the case of rough surfaces represented by means of smooth surfaces with equivalent dielectric constants determined by the scattering geometry and the electrical properties of the original rough surface, this approximation will not be acceptable. This is

due to the rather sensitive dependence of the surface constants to small changes in the value of the angle of incidence. However, as a first approximation, it is permissible to take the angles associated with the first, second and third modes of the smooth surface problem, use them to calculate the equivalent surface constants and solve the mode problem for the three modes in the rough-surface case. For a given mode, the surface constants are kept fixed as the duct width is varied. The numerical calculations which were performed indicate, however, that the angle of incidence of the mode varies with duct width so that it would be desirable to iterate the procedure so that the characteristic angle of elevation of a mode agrees with that used in calculating the equivalent constants of the rough surface. The effect of using surface constants which are not exact for the mode is not severe, however, as the actual attenuation rate differs from the approximate value by a few percent. For example, at $F_{rs} = 0.3$ and $K_1 = 10^{-7}$ per meter, we can see in figures 5.2 and 5.3 that attenuation rates for sea water and moist soil differ by approximately 11 percent. The following table shows how the characteristic angles of the first three modes in a duct having a linear refractive index profile change with mode order m. Information about the elevation angles of the various modes in a duct with infinite conductivity is valuable in solving the problem involving an imperfect

conductor for the lower wall of the guide.

Table 5.1. Elevation angles of duct modes.

Mode order	Elevation angle (millirad)	
	Sea water	Moist soil
1	4.8	4.8
2	6.4	6.4
3	7.4	7.4

This and knowledge of the real zeros of the Airy functions indicate the following procedure for finding the modes: Starting at a height which is adequate for supporting the desired mth mode, and using as the first trial zero the m-th zero of the appropriate Airy function, solve the mode equation using a Newton-Raphson procedure as described earlier. The duct depth will be incremented and the previous eigenvalue used as the first estimate of the solution (eigenvalue). By judiciously selecting the increment in duct depth, it is then possible to take advantage of the computational result that the eigenvalues lie along a line in the third quadrant

which tends to move away from the real axis as the duct depth is decreased toward zero. This procedure tends to reduce computation time as the eigenvalues can be reached in a few iterations of the Newton-Raphson routine.

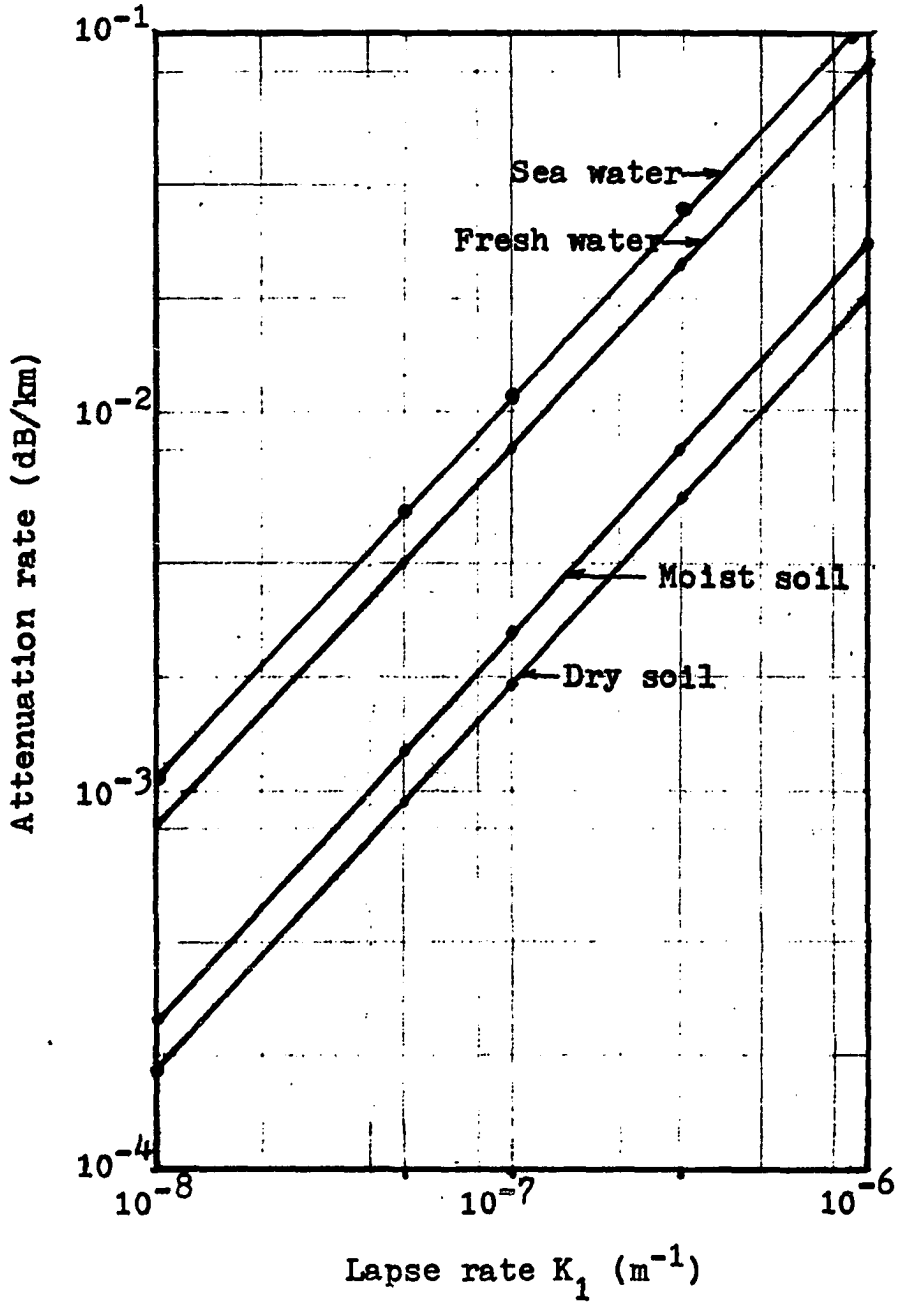

Figure 5.1. Attenuation rate vs. lapse rate for four smooth surfaces.

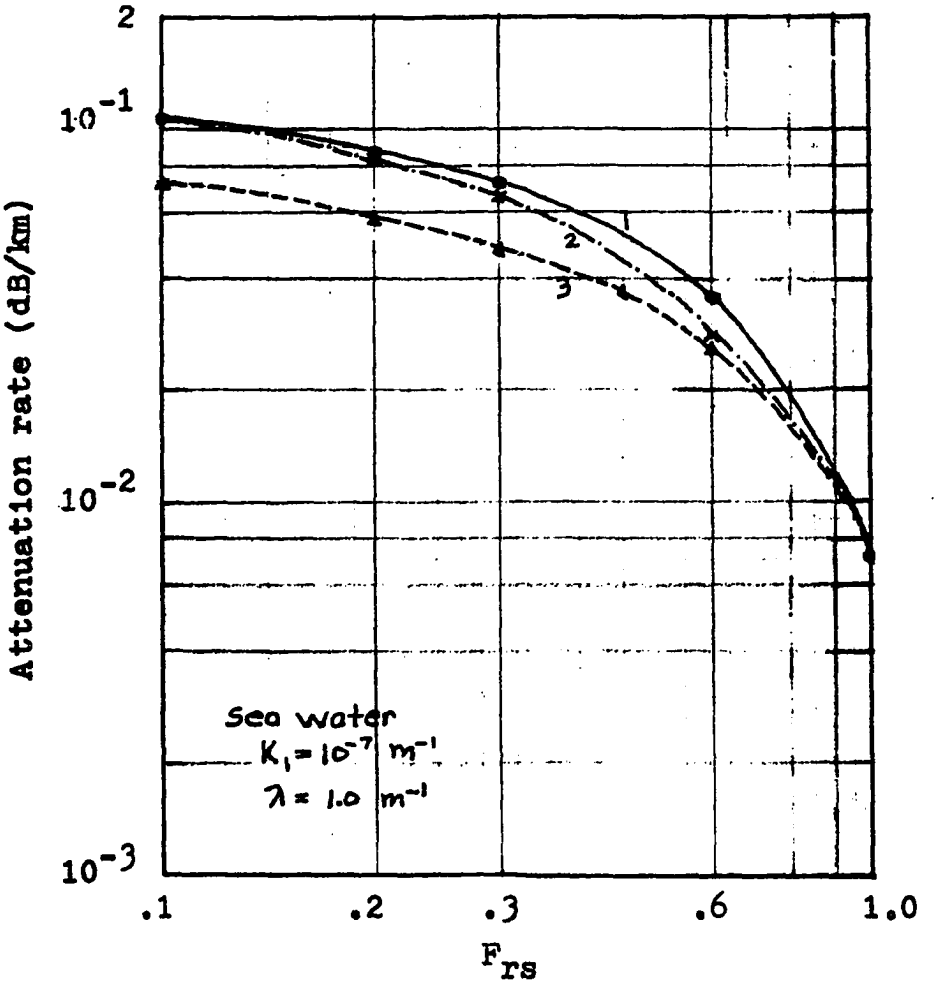

Figure 5.2. Attenuation rate vs. F_{rs} for the first three modes in a linear duct over sea water. $K_1 = 10^{-7}$ m^{-1}, $\lambda = 1.0$ m.

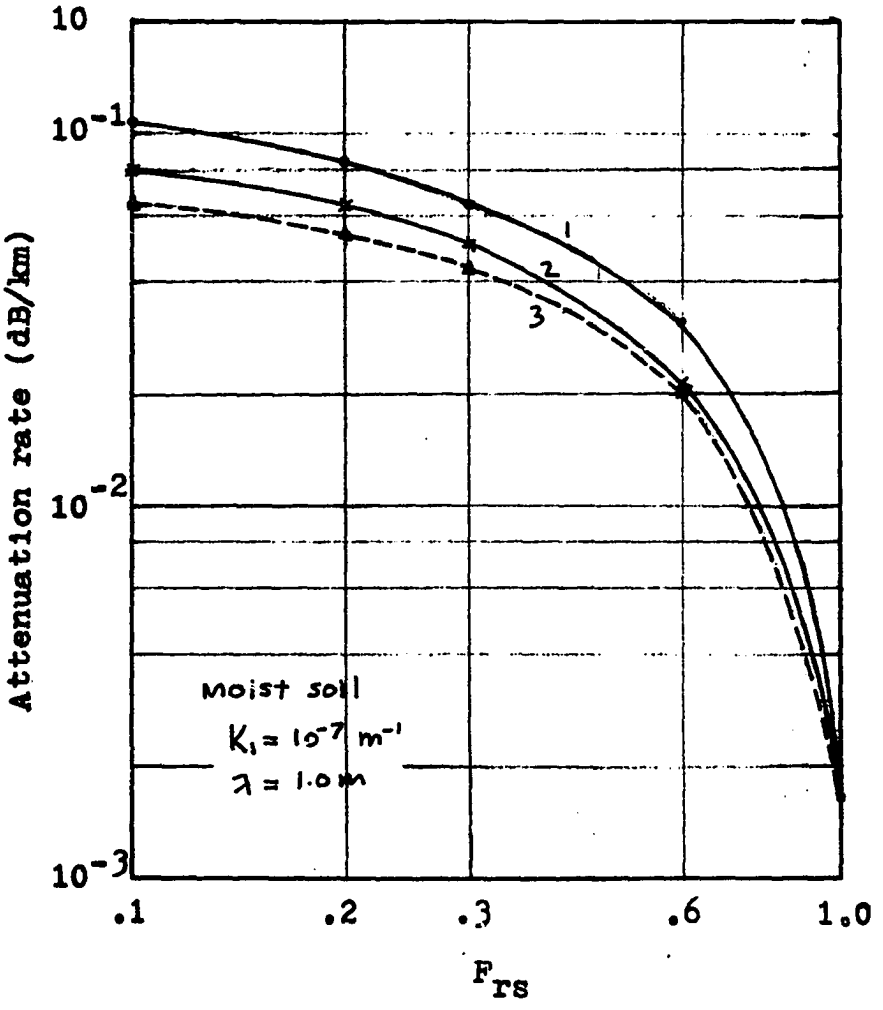

Figure 5.3. Attenuation rate vs. F_{rs} for the first three modes in a linear duct over moist soil. $K_1 = 10^{-7}$ m^{-1}, $\lambda = 1.0$ m.

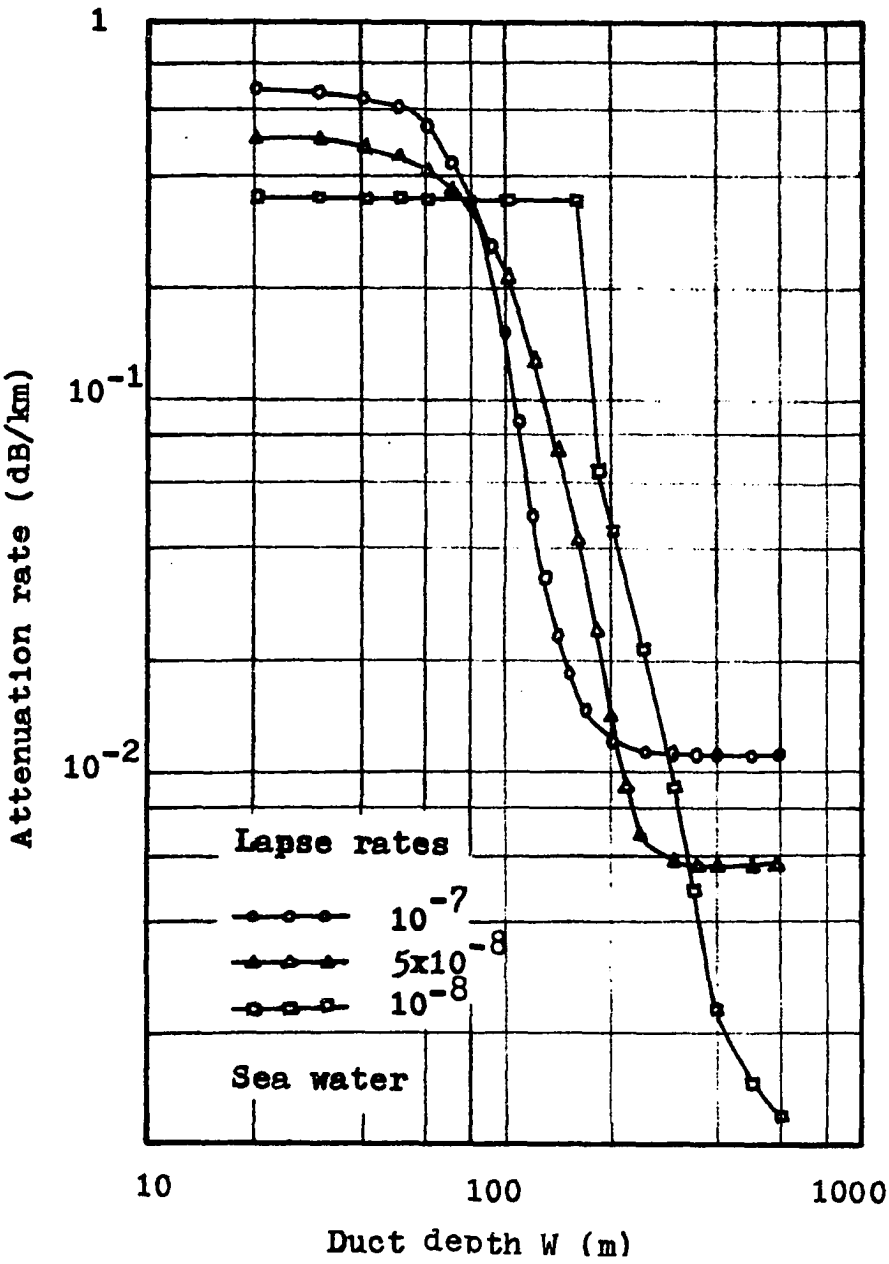

Figure 5.4. Comparative attenuation rates of the first modes in ducts with bilinear profiles over sea water for three lapse rates. Wavelength = 1.0 m.

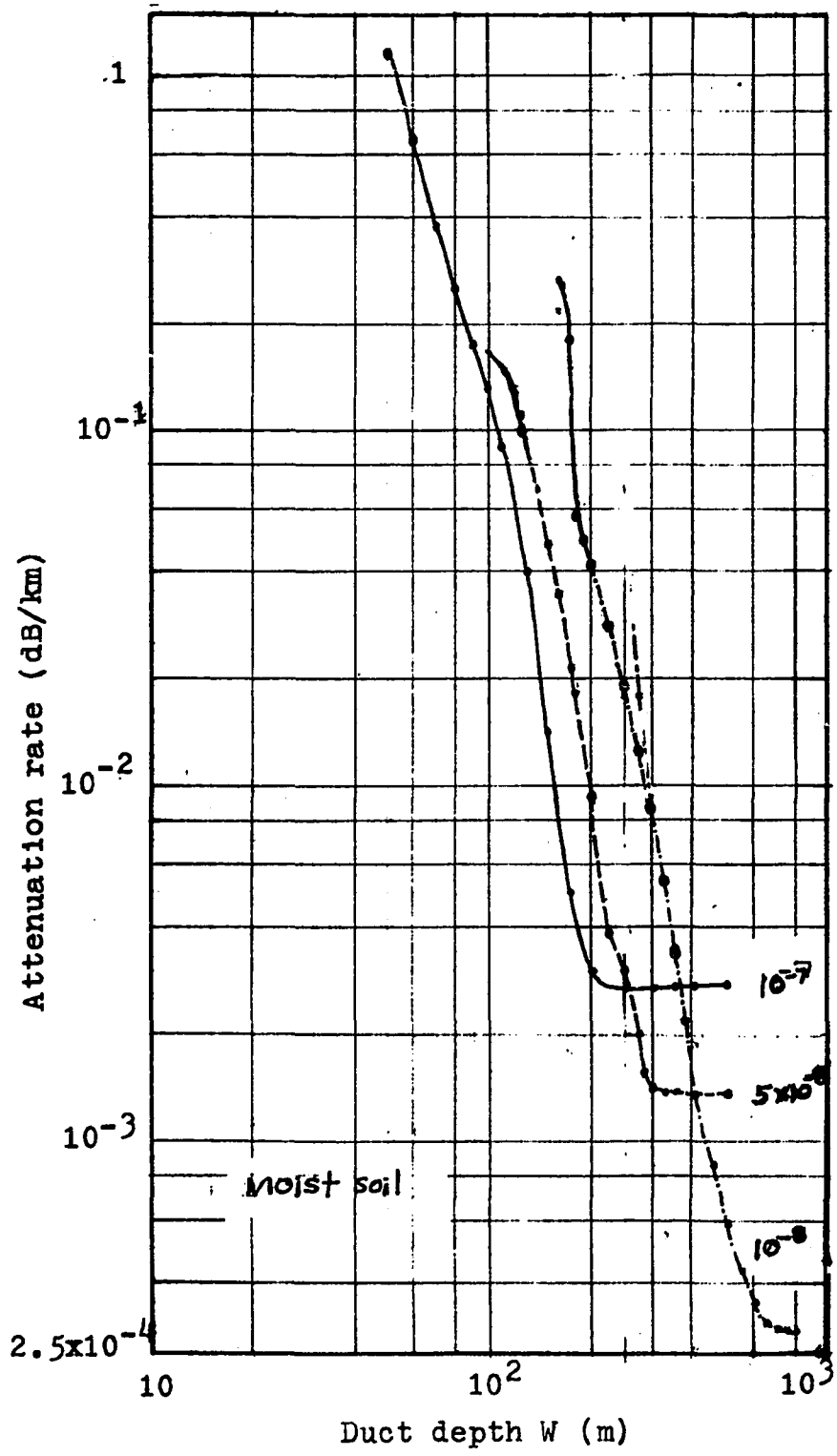

Figure 5.5. Comparative attenuation rates of the first modes in ducts with bilinear profiles over moist soil. Wavelength = 1.0 m.

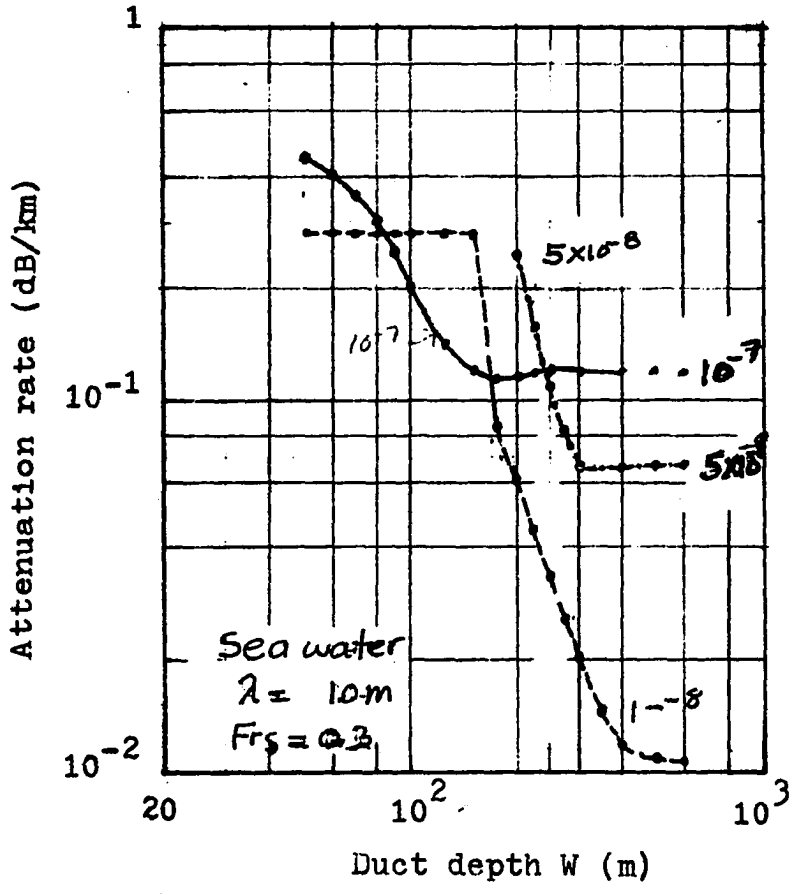

Figure 5.6. Comparative attenuation rates for first modes in ducts with bilinear profiles over rough sea water. $F_{rs} = 0.3$.

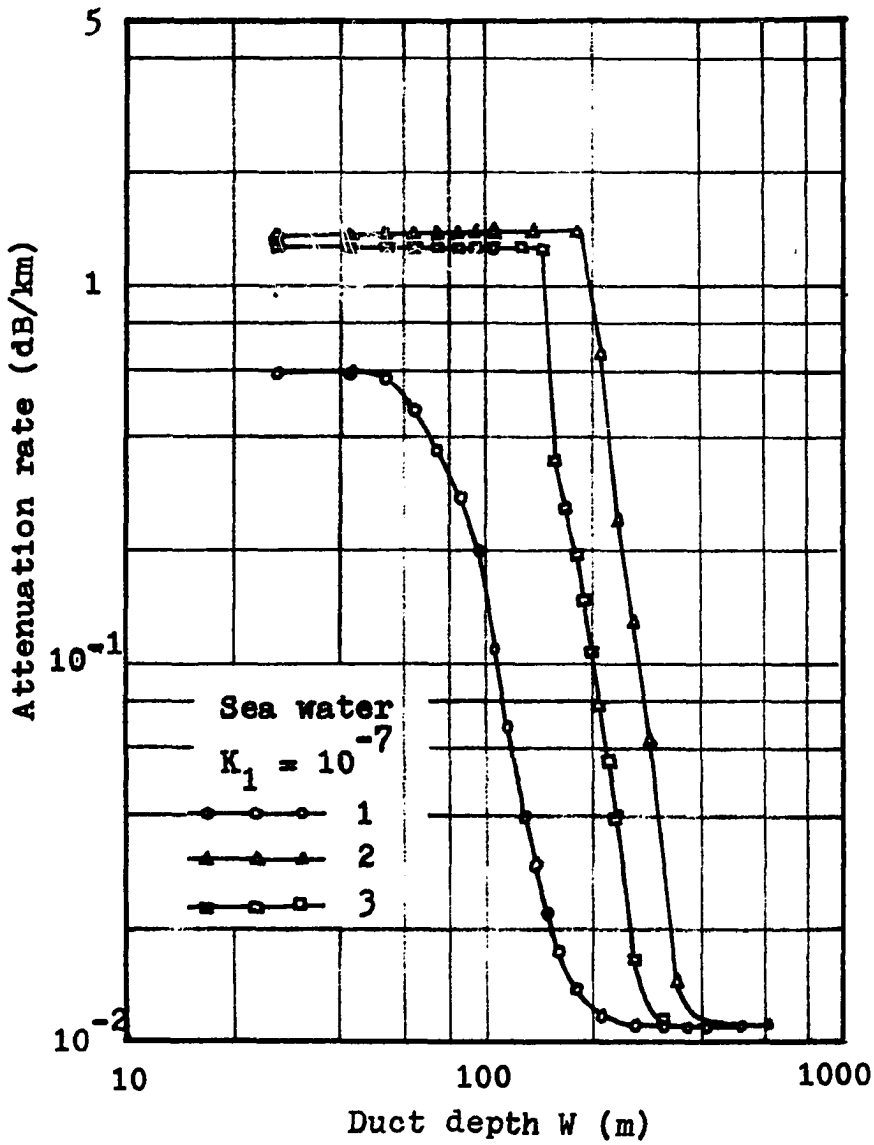

Figure 5.7. Attenuation rates of the first three modes in a duct with bilinear profile of refractive index over smooth sea. Wavelength = 1.0 m.

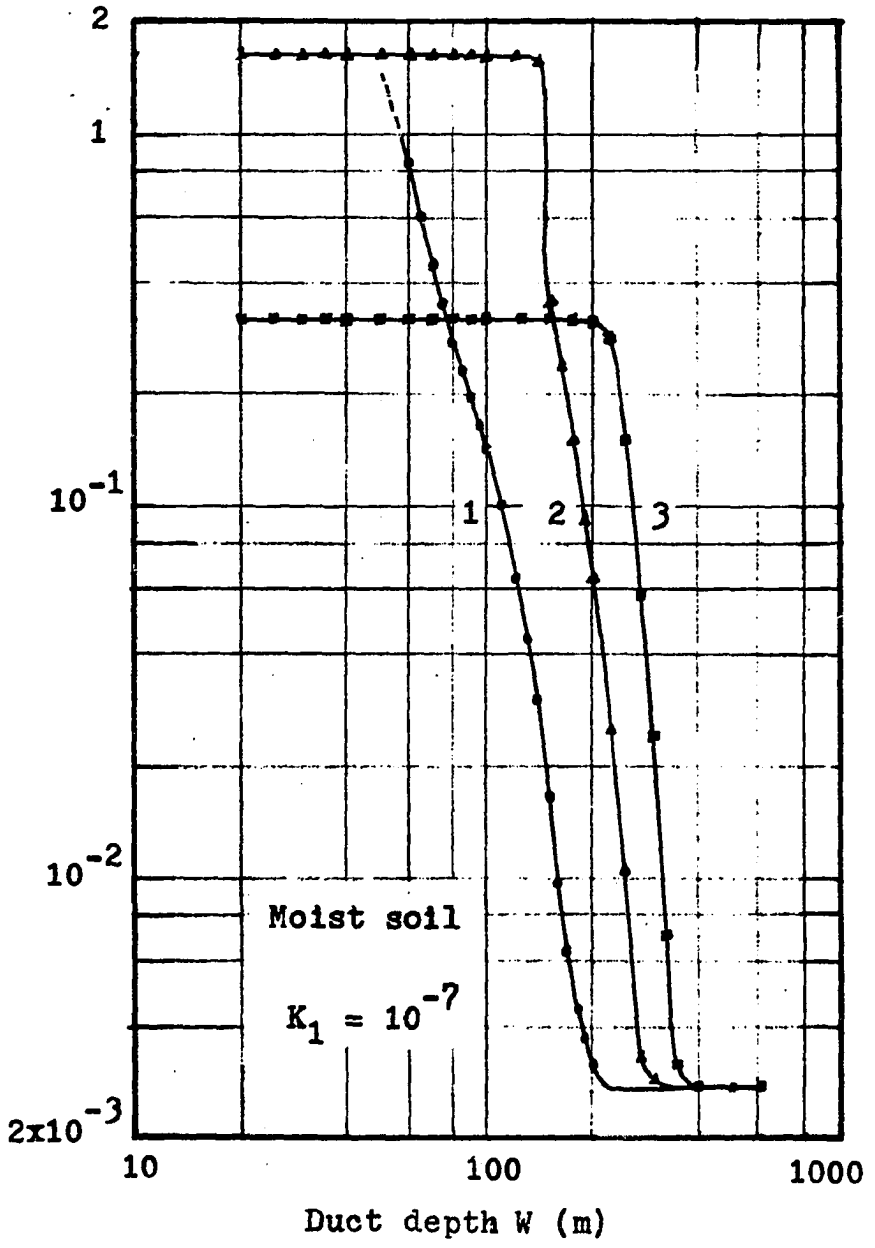

Figure 5.8. Attenuation rates of the first three modes in a duct with bilinear profile of refractive index over smooth moist soil. Wavelength = 1.0 m.

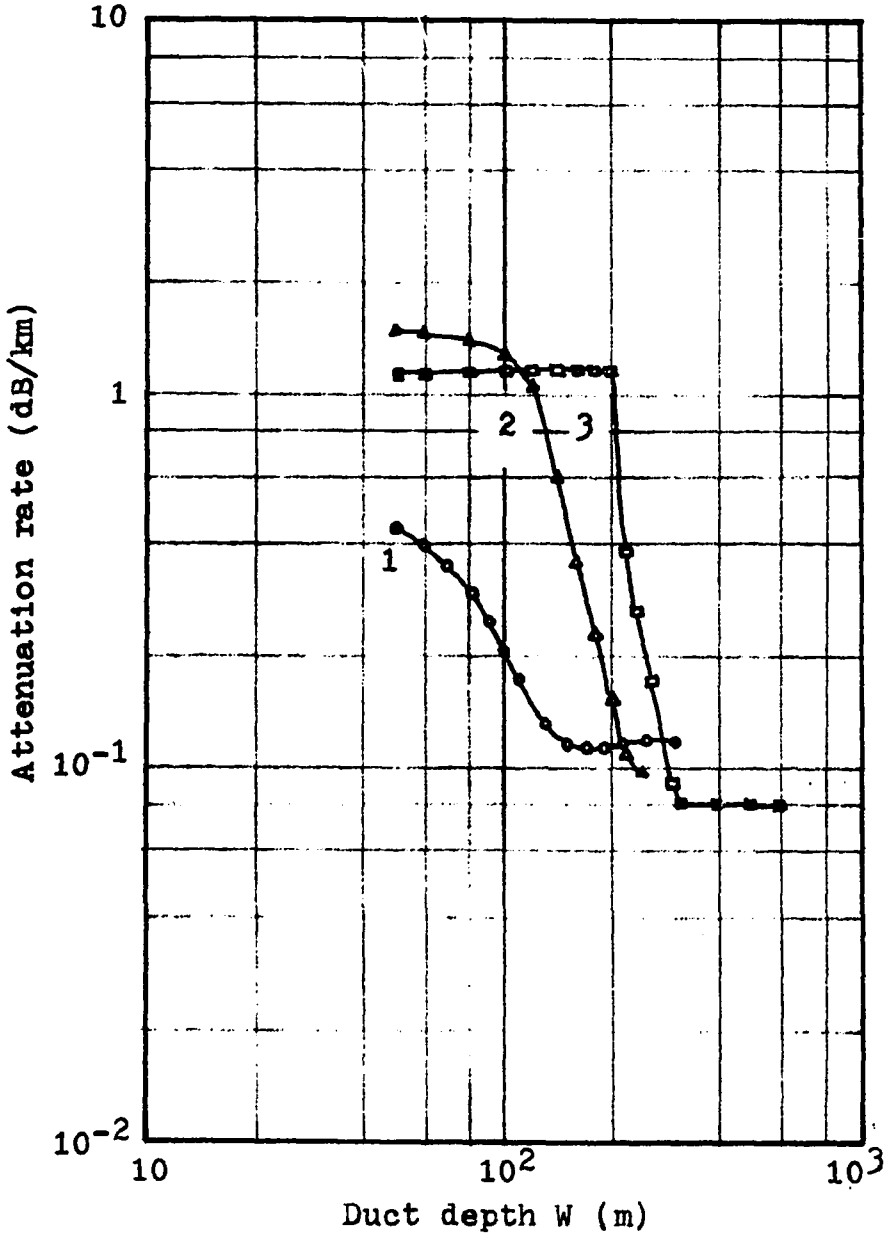

Figure 5.9. Attenuation rates of the first three modes in a bilinear duct over rough sea with F_{rs} = 0.3.

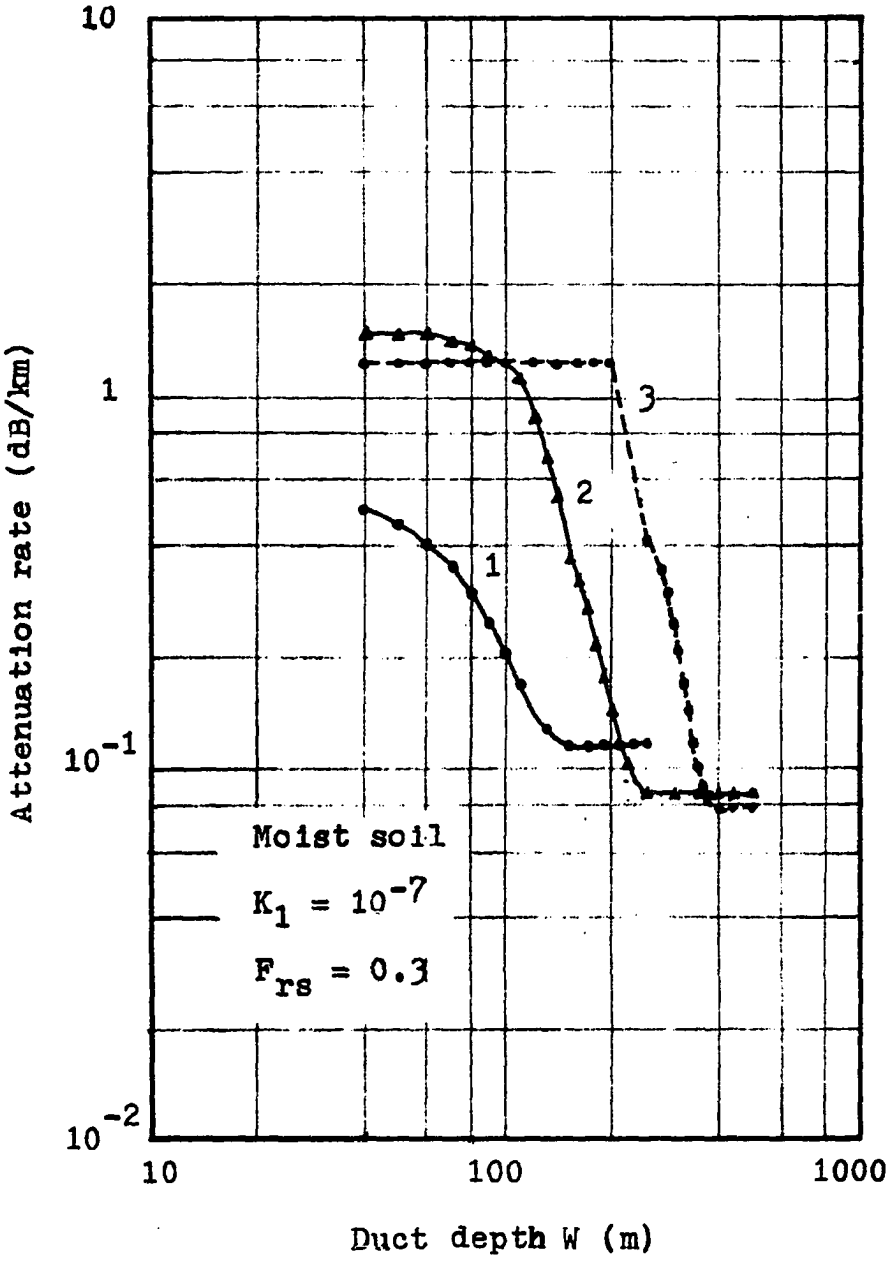

Figure 5.10. Attenuation rates of the first three modes in a bilinear duct over rough moist soil with $F_{rs} = 0.3$.

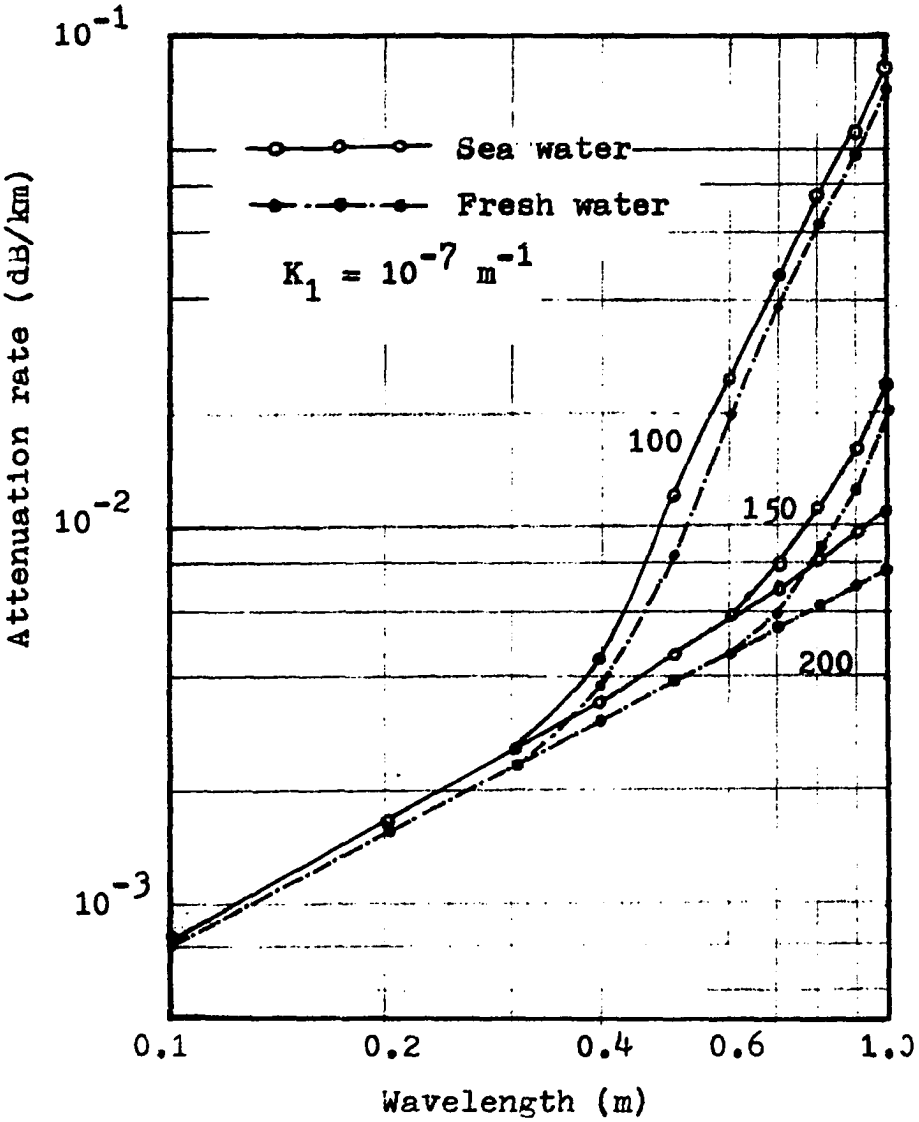

Figure 5.11. Attenuation rate vs. wavelength for sea and fresh water. Bilinear profile of refractive index. Duct depth is indicated by number near the curves.

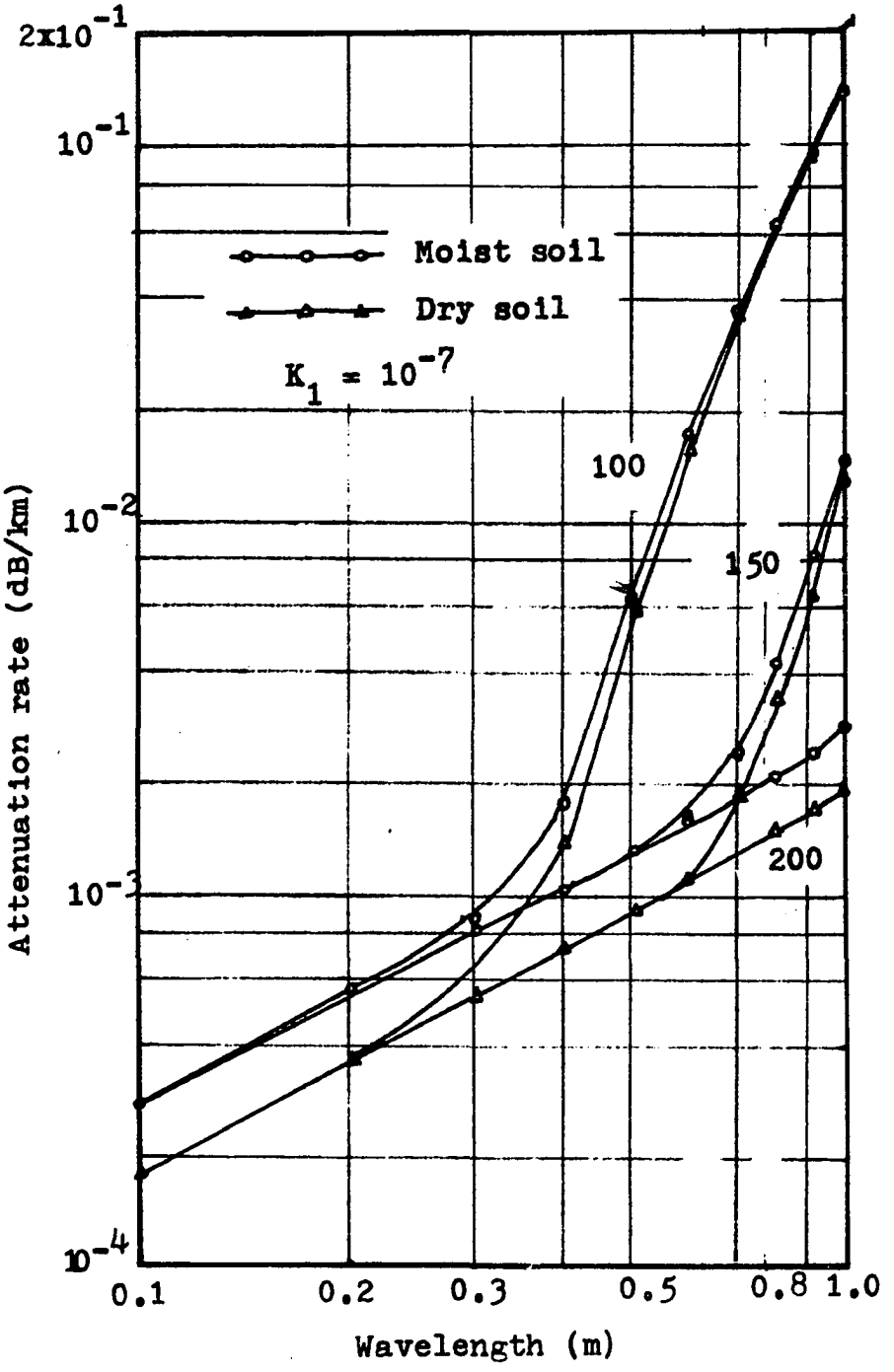

Figure 5.12. Attenuation rate vs. wavelength for moist and dry soil. Bilinear profile of refrac- index. Duct depth is indicated by number near the curves.

DISCUSSION

The results presented in the preceding chapter are admittedly based upon a limited number of examples, a consequence of the rather appreciable amount of computing time expended in developing the routines for evaluating the Airy integral function with complex argument. The choice of the range of lapse rates considered in the bilinear problem was dictated by the routine for evaluating the Airy integral function. It was decided at the time the data runs were made that the Airy integral function will be evaluated only when the argument has a modulus of about 9 units or less, which would call for a truncated power series expansion involving at the most forty-two terms in the third power of the complex argument u. This restriction on the modulus of the argument of the Airy integral function comes about because of the occurrence of arguments of the type

$$u_{11} = u_{10} - B_1' z_1 \tag{6.1}$$

for the bilinear problem.

It can be readily seen that for a lapse rate of 10^{-6} per meter and a duct height $z_1 = 100$ meters, the product $-B_1' z_1$ can range in magnitude from 1 to 10.

The procedure used in evaluating the power series expansion of the Airy integral function does not in all likelihood represent the optimum technique. There could be other non-standard methods for evaluating power series with complex arguments such that the precision inherent in the use of double precision can be fully utilized. Such techniques as scaling and translation come to mind and probably deserve a better examination for their possible application in problems of the type considered in this thesis. The results described below were obtained with the Airy integral function evaluation done in double precision arithmetic and with the series expansion of the function expressed in the nested form.

Linear profile over smooth surfaces. In looking at the graphs of the attenuation rates of the first mode in a duct with a linear profile of refractive index for smooth surfaces we discern the following patterns: (1) attenuation rate a increases with lapse rate over the range of values considered; (2) attenuation rate increases with the modulus of the complex dielectric constant $\varepsilon_r - j\sigma/\omega\varepsilon_o$; and (3) the graphs of the rate of attenuation for the modes are approximately the same for a given surface. Since the first two observations are applicable also to the bilinear case, their discussion will be deferred until after the results for the bilinear analysis have been examined. It is apparent that

when modes are wholly locked, in the sense that there is sufficient duct depth for supporting them, the attenuation rates are remarkably similar for the three modes considered. Upon examination, it turns out that this is a consequence of the approximation that the surface impedance of the ground does not change with the angle of incidence. As discussed earlier, this approximation works rather well when the modulus of the complex dielectric constant is appreciably greater than unity. The effect is of secondary importance since broad flat natural surfaces are seldom encountered under most propagation conditions. It is to be noted that the eigenvalues of the mode equation lie near the zeros of the first derivative of the Airy integral function Ai'(u).

Bilinear profile of refractive index. Next we look at the manner in which the attenuation rate of the first mode varies with lapse rate within the duct for the bilinear case. The next two sets of graphs depicts the manner in which attenuation rate changes with lapse rate for a given duct height. Here the results are consistent with those for the linear case in those cases in which the duct is sufficiently deep to support the modes. Thus it can be seen that the least attenuated first mode is that in the duct with the lowest lapse rate. The trend shown by the three curves for the first mode over smooth sea water at three different lapse

rates is that when the duct depth is sufficient, the lowest attenuation occurs when the lapse rate is least. Another interesting feature of this set of curves is that complete guiding does not occur at the same value of the refractive index contrast $\Delta n = K_1 z_1$, as indicated by the "knee" of the a vs. W curves. Instead, the apparent trend is that at higher lapse rates the contrast Δn is greater than that at low values of $K_1 z_1$. By comparison, the work of Wait and Spies (11) and also that of Chang (18) show that for elevated ducts equal attenuation occurs for equal contrast Δn. Note that a comparison between elevated and surface ducts is difficult to make in view of the different mechanisms causing mode attenuation. In the case of surface ducts, both ground dissipation and leakage through the top of the duct bring about energy loss, whereas for elevated ducts energy is lost only through leakage to regions above and below the duct.

At the other extreme, when quasi-propagating modes are indicated since the radio duct is not deep enough, the opposite behavior is observable, namely that attenuation decreases as lapse rate increases. Note that the duct depth has to be greater when the lapse rate is less; this is consistent with the requirement that a wave has to take a longer distance over which it can be refracted if the lapse rate is low. For ducts which do not have sufficient depth, the three modes experience differing degrees of attenuation, with the

lowest modes being attenuated least. Note also that at the limit when the duct depth is zero, the attenuation rate of the "modes" are those for smooth-earth diffraction. A possible explanation of this phenomenon is that when the lapse rate is small the duct must be relatively deep for bona fide modes to be supported. For a given amount of energy to be conveyed along the surfaced-based guide, the energy density within the duct varies inversely with duct depth. Thus it seems reasonable that the electrical field at the air-ground interface must be lower and consequently the attendant conduction loss in the surface material is less than would be case if the duct were shallower.

The foregoing discussion might be compared with the theoretical prediction for the rate of attenuation in a rectangular waveguide. In Brown et al. (21, p.262), for example, we will find that the rate of attenuation for a field in the TE mode inside a rectangular guide is inversely proportional to the crossguide dimensions.

The modes in ducts having the same refractive index profile may be compared when the lower boundaries have different electrical properties. The trend that can be observed is that the surface having lower conductivity supports modes which are attenuated less than those in a duct over a relatively better conductor. This agrees with the results

obtained for the linear-profile ducts.

Finally, Figures 5.11 and 5.12 show how the attenuation rate of the first mode in a duct with a given refractive index profile varies with the wavelength of the field inside the duct. The data for three duct heights show the common trend that the rate of attenuation per unit distance in the direction of propagation varies directly with wavelength: the longer the wavelength, the higher the attenuation, the longer wavelengths seemingly exhibiting a greater tendency to leak through the upper region of the duct. The curves for sea and fresh water track rather well, especially at short wavelengths. This trend can be ascribed to the manner in which the factor

$$q = -jk/(\varepsilon_r - j\sigma/\omega\varepsilon_o)^{1/2}$$

varies with wavelength.

CONCLUSIONS

This work was intended to incorporate the effects of surface roughness and the finite conductivity of the ground in the formulation of the waveguide-mode propagation problem for surface-based tropospheric ducts. The concept of a scalar rough-surface reflection factor F_{rs}, based upon the principal effect of surface roughness, namely diffuse scattering and the attendant reduction of the observed field, was introduced. By this procedure, a rough contour can be replaced with an equivalent imperfectly conducting plane, the electromagnetic properties of which are determined by those of the assumed homogeneous rough surface and the factor F_{rs}.

Calculations based on typical surface duct parameters showed some rather significant results. First, in contrast with previous assumptions, modes over relatively "good" conducting surfaces are attenuated more, not less, than those over "poorly" conducting surfaces. Second, surface roughness causes an important change in mode attenuation: the rougher a surface is, the higher the attenuation of a mode. Also, for sufficiently rough surfaces, such as those with F_{rs} of approximately 0.3 or less, the difference between the attenuation curves for different materials is relatively small.

The results described earlier suggest some areas for possible investigation. One of these has to do with the

mechanism for long-range radio propagation via radio ducts. Since the results show in part that a good conductor such as the sea causes a higher rate of attenuation in a wave propagating over it, long-range propagation under inversion conditions must be accounted for by some mechanism other than that involving the sea or ground as a boundary of the duct. Information concerning the manner in which the mode properties are affected by the surface reflection factor, and more realistic, and often more complicated, profiles of refractive index should be examined. One interesting case would be to study the ES duct (elevated layer, surface duct) in order that we might determine whether long-distance propagation is best supported in an elevated layer or within a surface-based duct. It should be stressed that the ES duct referred to here is different from the elevated ducts studied by Wait and Spies(12) and Chang(13) (see figure 1.2).

In any proposed application of the linear-segmented profile method for radio ducts, a serious disadvantage is present in the power-series expansion of the Airy integral function. Other techniques for solving the mode equation should be studied so that the full potential of the method used in the present work can be realized. Analog computation techniques should be examined and, if found to yield results faster and relatively inexpensively, the method could be considered for such applications as remote-sensing of the

troposphere, propagation path prediction, etc. Accordingly, the next step to take is to find more powerful means for solving the waveguide-mode problem, especially for cases where the refractive index profile has to be more accurately represented by many linear segments. Hopefully, we might see some potential contributions being made in the areas of radiowave propagation mechanisms in the troposphere and in remote sensing in the atmosphere.

BIBLIOGRAPHY

1. Watson, G. N. "The diffraction of electric waves by the earth." Proc. Roy. Soc. A 95, No. A666 (October, 1918): 83-99.

2. Watson, G. N. "The transmission of electric waves round the earth." Proc. Roy. Soc. A 95, No. A673 (July, 1919): 546-563.

3. Kerr, D. E. Propagation of short radio waves. New York: McGraw-Hill, 1951.

4. Booker, H. G.; and W. Walkinshaw. "The mode theory of tropospheric refraction and its relation to wave-guides and diffraction." Report: Meteorological Factors in Radio Wave Propagation. London: Physical Society, 1948.

5. Eckersley, T. L. "Radio transmission problems treated by phase integral methods." Proc. Roy. Soc. A, A 133 (June, 1932): 499-527.

6. Eckersley, T. L.; and G. Millington. "Application of the phase integral method to the analysis of the diffraction and refraction of wireless waves round the earth." Phil. Trans. Roy. Soc. A 237 (June, 1938): 273-309.

7. Budden, K. G. The Waveguide-Mode Theory of Wave Propagation. Englewood Cliffs, N.J.: Prentice-Hall, 1960.

8. Pekeris, C. L. "Accuracy of the earth-flattening approximation in the theory of microwave propagation." Phys. Rev. 70, No. 7 (October 15, 1946): 518-522.

9. Bean, B. R.; and E. J. Dutton. Radio Meteorology. Washington, D.C.: U.S. Natl. Bur. Stand., 1966.

10. du Castel, F. Tropospheric Radiowave Propagation Beyond the Horizon. Oxford: Pergamon, 1966.

11. Wait, J. R. Electromagnetic Waves in Stratified Media. New York: Pergamon, 1970.

12. Wait, J. R.; and K. Spies. "Internal guiding of microwaves by an elevated tropospheric layer." Rad. Sci. 4, No. 4 (April, 1969): 319-326.

13. Chang, H.-C. "The effects of tropospheric layer structures on long-range VHF radio propagation." IEEE Trans. Antennas Propag. AP-19, No. 6 (November, 1971): 751-756.

14. T. B. A. Senior. "Impedance boundary conditions for imperfectly conducting surfaces." Appl. Sci. Res. Sec. B, 8 (1960): 418-436.

15. T. B. A. Senior. "Impedance boundary conditions for statistically rough surfaces." Appl. Sci. Res. Sec. B, 8 (1960): 437-462.

16. Gerks, I.; and R. M. Anderson. "Diffraction of radio waves in a stratified troposphere." Rad. Sci. 1, No. 8 (August, 1966): 897-912.

17. Miller, J. C. P. The Airy Integral. Cambridge: University Press, 1946.

18. Abramowitz, M.; and I. Stegun (Eds.). Handbook of Mathematical Functions. Washington, D. C.: U. S. Natl. Bur. Stand., 1964.

19. Young, D. M.; and R. T. Gregory. A Survey of Numerical Mathematics. Vol. 1. Reading, Mass.: Addison-Wesley, 1972.

20. Silver, S. (Ed.). Microwave Antenna Theory and Design. New York: Dover, 1965.

21. Brown, R. G.; R. A. Sharpe; W. L. Hughes; and R. E. Post. Lines, Waves, and Antennas. New York: Ronald, 1973.

ACKNOWLEDGEMENT

The author wishes to express his appreciation for the valuable help that his major professor, Dr. Robert E. Post, gave throughout the conduct of this work, from the ideas which led to the selection of the subject to the suggestions, questions, comments and criticisms while the author struggled with the problem. The financial support received by the author from the University of the Philippines and Educational Projects, Inc. while he was at Iowa State University is hereby gratefully acknowledged. The encouragement and support of friends at Iowa State is also acknowledged.

This work is dedicated to my long-suffering wife, Athena, and our daughter Vivienne.

APPENDIX: COMPUTER PROGRAM LISTING

```
C*****PROGRAM TO FIND THE MODES IN A DUCT WITH A BILINEAR
C*****PROFILE OF REFRACTIVE INDEX.
C*****THE FOLLOWING NOTATION IS USED IN THE PROGRAM:
C
C      Z        STARTING VALUE OF THE SOLUTION
C      Z1       DUCT WIDTH IN METERS
C      RE       RELATIVE PERMITTIVITY
C      RX       X = 60 X CONDUCTIVITY X WAVELENGTH
C      WL       WAVELENGTH
C      ZQ       GROUND CONSTANT
C      CM       MODE EQUATION
C      FM       FIRST DERIVATIVE OF THE MODE EQUATION
C      ZANG     MODE ANGLE
C      ZTHETA   SOLUTION OF THE MODE EQUATION
C
C     AS GIVEN HERE, THE PROGRAM CALCULATES THE COMPLEX MODE
C     ANGLE "ZTHETA" FOR A SPECIFIED RANGE OF VALUES OF
C     DUCT HEIGHTS "Z1".   THE RANGE IS FROM
C     "Z1" TO "RLIM" AT STEPS OF "RDEL".
C      TO USE THIS PROGRAM FOR A LINEAR PROFILE OF REFRACTIVE
C     INDEX, THE PROGRAM IS SLIGHTLY MODIFIED SINCE THE MODE
C     EQUATION FOR THIS CASE IS SIMPLER.
C     THE FOLLOWING STEPS REPLACE THOSE STARTING WITH THE
C     U1 = Z STATEMENT UP TO Z = Z - CM/FM
C
C*************************************************************
C*************************************************************
      CALL AI1(Z,AI,IZ)
      CALL AI2(Z,AA,IZ)
      CM = -B1*AA + ZQ*AI
      IF(CDABS(CM).LE.DERR) GO TO 666
C     OTHERWISE, FIND NEW ESTIMATE USING NEWTON'S METHOD
      FM = -B1*Z*AI + ZQ*AA
      IF(CDABS(FM)LE.DERR) GO TO 555
C     IF NOT, CALCULATE NEW Z
      Z = Z - CM/FM
C*************************************************************
C*************************************************************
C
C     MAIN PROGRAM   MAIN PROGRAM
C
      IMPLICIT COMPLEX*16(A-C,F,U-Z),REAL*8(D,R)
      COMPLEX*16 DCMPLX,DCONJG
      REAL*8 RL(5)
      COMPLEX*16 ZIN(5)
      REAL*8 CDABS
```

```
      REAL*8 B1,B2,BK,CI
      REAL*4 CMR,CMI,DA,DB,DC,ABS
      ERR = 1.E-4
      DATA ZJ/(0.D0, 1.D0)/
      READ,RE,RX,RLMDA,RL1,RL2
      READ,Z1,Z
      WRITE(6,13)
   13 FORMAT('1')
      ZS=Z
      DPI = .3141592653589793D1
      DERR = 1.D-6
      RL2 = 1.25E-7
      DP2 = DPI*DPI
      DK2 = .40D1*DP2/RLMDA**2
      ZREAL = (1.D0,0.0D0)
      CI = DSQRT(3.D0)/2.D0
      ZU = DCMPLX(-.5D0,-CI)
      CJ = (0.,1.)
      E=10
      S=.01
      WL= 1.
C     CALCULATE VALUES OF U10,U11,U21 AT LEVELS Z=/ AND Z = Z1
      I = 1
      J = 1
      ZQ = (-ZJ*.20D1*DPI/RLMDA)/CDSQRT(DCMPLX(RE,-RX))
      D3 = 1.D0/3.D0
      B1 = -((DK2*2.D0*RL1)**D3)
      B2 =   (DK2*2.D0*RL2)**D3
      BK = -B2*RL1/(B1*RL2)
      CM1 = 0.
    7 CALL ZSIZE(Z,IZ)
      IF(I.GT.20) GO TO 666
C*************************************************************
C*************************************************************
C     START OF THE CALLING ROUTINE FOR BILINEAR PROFILE PROBLEM
      U1=Z
      US = U1
      V1=U1*ZU
      U2 = U1 - B1*Z1
      V2 = U2*ZU
      V3 = ZU*( U1*BK + B2*RL1*Z1/RL2)
      CALL AI2(V1,BP10,IZ)
      CALL AI1(U2,A11,IZ)
      CALL AI2(U2,AP11,IZ)
      CALL AI1(V3,B21,IZ)
      CALL AI1(V2,B11,IZ)
      CALL AI2(V3,BP21,IZ)
      CALL AI2(V2,BP11,IZ)
      CALL AI2(U1,AP10,IZ)
      CALL AI1(U1,A10,IZ)
```

```
      CALL AI1(V1,B10,IZ)
C*****FORM THE MODE EQUATION CM***
C
      CX = -B2*ZU*BP21
      CY = B21
      CW = B11*CX + B1*ZU*BP11*CY
      CT = A11*CX + B1*AP11*CY
      CP = -B1*AP10+ZQ*A10
      CR = -B1*ZU*BP10 + ZQ*B10
      CM(MM,KK) = -(CW*CP/CT) + CR
      PRINT,I,U1,CM
            IF(CDABS(CM).LE.DERR) GO TO 666
C*****A NEW ESTIMATE OF THE POINT "U1)
      CXP = ZU*ZU*(-B2)*B21*V3
      CYP = BP21*ZU*BK
      CWP = BP11*ZU*CX + B11*CXP
     1 +  B1*ZU*(B11*V2*ZU*CY + BP11*CYP)
      CTP = AP11*CX + A11*CXP + B1*(U2*A11*CY + AP11*CYP)
      CPP = -B1*U1*A10 + ZQ*AP10
      CRP =(-B1*ZU*V1*B10 + ZQ*BP10)*ZU
      FM = (-(CT*CWP - CW*CTP)*CP/(CT*CT)) - (CW/CT)*CPP + CRP
      PRINT,I,FM
      PRINT,CWP,CPP,CTP,CRP
      DFM=CDABS(FM)
      IF(DFM.LE.DERR) GO TO 555
C**************************************************************
C**************************************************************
C     THIS ENDS THE SECTION OF THE PROGRAM FOR USE IN SOLVING
C     THE MODE PROBLEM FOR THE DUCT WITH BILINEAR PROFILE
      Z = Z - CM/FM
      REALZ = ZREAL*Z
      IF(REALZ.GT.1.0D0) GO TO 333
      I=I+1
      GO TO 7
  333 Z = ZS-.5D0
      ZS = Z
      I=I+1
      GO TO 7
  555 Z=Z-.1D0
      I=I+1
      GO TO 7
  666 PRINT,I,Z,CM(MM,KK)
      PRINT,LZ,IX,Z1,RX
C     FIND THE MODE ANGLE
      ZC2 = 1.0D0 - Z*2.0D0*RL1/B1
      ZTHETA = CDSQRT(ZC2)
      PRINT,ZC2,ZTHETA
C     CALCULATE THE COMPLEX MODE ANGLE
      ZANG = -ZJ*CDLOG(ZTHETA + CDSQRT(ZC2-1.0D0))
C**** CHECK IF THE COMPUTED VALUE OF ZANG IS CORRECT
```

```
      ZTH = CDCOS(ZANG)
      WRITE(6,17) ZANG,ZTH
   17 FORMAT(' ','ZANG = ',5X,D28.16,5X,D28.16,  /,
     2'(COS(ZTH) = ',  5X,D28.16,5X,D28.16)
      WRITE(6,31)
   31 FORMAT('0',/////)
  777 CONTINUE
      STOP
      END
C
C
C
      SUBROUTINE AI1(Z,ZAI,K)
      IMPLICIT COMPLEX*16(Z)
      COMPLEX*16 F(50),G(50), DCMPLX
      REAL*8 DSQRT,CA,CB
      DATA CA,CB/.355028053887817, .258819403792807/
      ZU=DCMPLX(-.5D0,-DSQRT(3.D0)/2.D0)
      Z3=Z**3
      L=3*K
      F(K) =1.D0 +Z3/(L*(L-1))
      G(K) = 1.D0 + Z3/(L*(L-1))
      M=K-1
      DO 90 I=1,M
      J= K-I
      N=3*J
      F(J) = 1.D0+F(J+1)*(Z3/(N*(N-1)))
      G(J) = 1.D0+G(J+1)*(Z3/(N*(N+1)))
      IF(J.GT.1) GO TO 90
      IF(J.EQ.1) GO TO 20
      GO TO 90
   20 ZAI=CA*F(1)-CB*G(1)*Z
   90 CONTINUE
   99 CONTINUE
      RETURN
      END
C
C
C
      SUBROUTINE AI2(Z,ZAA,K)
      IMPLICIT COMPLEX*16(Z)
      COMPLEX*16 F(50),G(50), DCMPLX
      REAL*8 DSQRT,CA,CB
      II=1
      DATA CA,CB/.355028053887817, .258819403792807/
      Z3=Z**3
      L=3*K
      F(K)=1.D0+Z3/((L-1)*(L-3))
      G(K)=1.D0+Z3/(L*(L-2))
      M=K-2
```

```
      DO 90 I=1,M
      J=K-I
      N=3*J
      F(J) = 1.D0 + F(J+1)*(Z3/((N-1)*(N-3)))
      G(J) = 1.D0 + G(J+1)*(Z3/ (N*(N-2)))
      IF(J.EQ.2) GO TO 20
      GO TO 90
   20 F(1) = F(2)*(Z*Z /2.D0 )
      G(1) =  1.D0 + G(2)*(Z3/3.D0)
      ZAA = CA*F(1) - CB*G(1)
   90 CONTINUE
   99 CONTINUE
      RETURN
      END
C
C
C
      SUBROUTINE ZSIZE(Z,IZ)
      COMPLEX*16 Z
      REAL*8 RZ,CDABS
      RZ = CDABS(Z)
      IF(RZ.LE.2.0D0) GO TO 41
      IF(RZ.LE.4.0D0) GO TO 42
      IF(RZ.LE.5.0D0) GO TO 43
      IF(RZ.LE.6.0D0) GO TO 44
      IF(RZ.LE.7.0D0) GO TO 45
      IF(RZ.LE.8.0D0) GO TO 46
      IF(RZ.LE.9.0D0) GO TO 47
   41 IZ=12
      GO TO 7
   42 IZ=18
      GO TO 7
   43 IZ=22
      GO TO 7
   44 IZ=26
      GO TO 7
   45 IZ=30
      GO TO 7
   46 IZ=34
      GO TO 7
   47 IZ=42
    7 RETURN
      END
```